

An Adamantyl-Substituted Retinoid-Derived Molecule That Inhibits Cancer Cell Growth and Angiogenesis by Inducing Apoptosis and Binds to Small Heterodimer Partner Nuclear Receptor: Effects of Modifying Its Carboxylate Group on Apoptosis, Proliferation, and Protein-Tyrosine Phosphatase Activity

Marcia I. Dawson,^{*,†} Zebin Xia,[†] Gang Liu,[†] Joseph A. Fontana,[‡] Lulu Farhana,[‡] Bhamik B. Patel,[‡] Sankari Arumugarajah,[‡] Mohammad Bhuiyan,[‡] Xiao-Kun Zhang,[†] Young-Hoon Han,[†] William B. Stallcup,[§] Jun-ichi Fukushi,^{§,||} Tomas Mustelin,[⊥] Lutz Tautz,[⊥] Ying Su,[†] Danni L. Harris,[#] Nahid Waleh,[▽] Peter D. Hobbs,[▽] Ling Jong,[▽] Wan-ru Chao,[▽] Leonard J. Schiff,[◆] and Brahma P. Sani[∞]

Cancer Center, Burnham Institute for Medical Research, La Jolla, California 92037, Wayne State, University School of Medicine and Department of Veterans Affairs, Detroit, Michigan 48201, Molecular Research Institute, Mountain View, California 94043, Southern Research Institute, Birmingham, Alabama 35025, IIT Research Institute, Chicago, Illinois 60616, and SRI International, Menlo Park, California 94025

Received November 16, 2006

Apoptotic and antiproliferative activities of small heterodimer partner (SHP) nuclear receptor ligand (*E*)-4-[3'-(1-adamantyl)-4'-hydroxyphenyl]-3-chlorocinnamic acid (3-Cl-AHPC), which was derived from 6-[3'-(1-adamantyl)-4'-hydroxyphenyl]-2-naphthalenecarboxylic acid (AHPN), and several carboxyl isosteric or hydrogen bond-accepting analogues were examined. 3-Cl-AHPC continued to be the most effective apoptotic agent, whereas tetrazole, thiazolidine-2,4-dione, methylidinitrile, hydroxamic acid, boronic acid, 2-oxoaldehyde, and ethyl phosphonic acid hydrogen bond-acceptor analogues were inactive or less efficient inducers of KG-1 acute myeloid leukemia and MDA-MB-231 breast, H292 lung, and DU-145 prostate cancer cell apoptosis. Similarly, 3-Cl-AHPC was the most potent inhibitor of cell proliferation. 4-[3'-(1-Adamantyl)-4'-hydroxyphenyl]-3-chlorophenyltetrazole, (2*E*)-5-{2-[3'-(1-adamantyl)-2-chloro-4'-hydroxy-4-biphenyl]-ethenyl}-1*H*-tetrazole, 5-{4-[3'-(1-adamantyl)-4'-hydroxyphenyl]-3-chlorobenzylidene}thiazolidine-2,4-dione, and (3*E*)-4-[3'-(1-adamantyl)-2-chloro-4'-hydroxy-4-biphenyl]-2-oxobut-3-enal were very modest inhibitors of KG-1 proliferation. The other analogues were minimal inhibitors. Fragment-based QSAR analyses relating the polar termini with cancer cell growth inhibition revealed that length and van der Waals electrostatic surface potential were the most influential features on activity. 3-Cl-AHPC and the 3-chlorophenyltetrazole and 3-chlorobenzylidenethiazolidine-2,4-dione analogues were also able to inhibit SHP-2 protein-tyrosine phosphatase, which is elevated in some leukemias. 3-Cl-AHPC at 1.0 μ M induced human microvascular endothelial cell apoptosis but did not inhibit cell migration or tube formation.

Introduction

In investigating the effects of retinoids on cancer cell proliferation, we first noticed that the retinoid 6-[3'-(1-adamantyl)-4'-hydroxyphenyl]-2-naphthalenecarboxylic acid (AHPN/*CD437*, **1** in Figure 1)^{1,2} displayed the atypical functions of

* Address correspondence to Dr. Marcia I. Dawson, Burnham Institute for Medical Research, 10901 North Torrey Pines Rd., La Jolla, California 92037. Phone: 858-646-3165. Fax: 858-646-3197. E-mail: mdawson@burnham.org.

[†] Cancer Center, Burnham Institute for Medical Research.

[‡] Wayne State University School of Medicine and Department of Veterans Affairs.

[§] Neuroscience and Aging Center, Burnham Institute for Medical Research.

^{||} Present address: Kyushu University Hospital, Fukuoka City, Japan.

[⊥] Inflammatory and Infectious Disease Center, Burnham Institute for Medical Research.

[#] Molecular Research Institute.

[▽] SRI International.

[◆] IIT Research Institute (retired).

[∞] Southern Research Institute.

^a Abbreviations: 3-Cl-AHPC, (*E*)-4-[3'-(1-adamantyl)-4'-hydroxyphenyl]-3-chlorocinnamic acid; AHPN, 6-[3'-(1-adamantyl)-4'-hydroxyphenyl]-2-naphthalenecarboxylic acid; AML, acute myelocytic leukemia; DR5-*ik*-CAT, synthetic gene of retinoic acid response element of two direct repeats separated by five base pairs linked to the thymidine kinase promoter followed by the base sequence for chloramphenicol acetyl transferase gene; HMVE, human microvascular endothelial; RAR, retinoic acid receptor; RXR, retinoid X receptor; TTNC, (*E*)-4-(5',6',7',8'-tetrahydro-5',8',8'-tetramethyl-2'-naphthalenyl)cinnamic acid; TTNN, 6-(5',6',7',8'-tetrahydro-5',5',8',8'-tetramethyl-2'-naphthalenyl)-2-naphthalenecarboxylic acid.

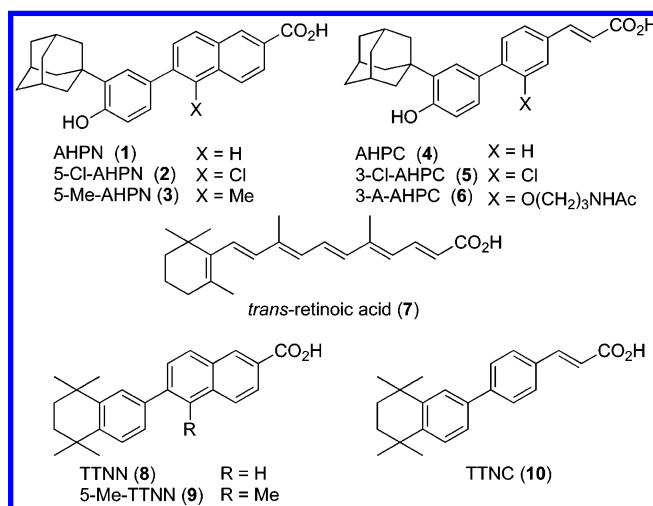


Figure 1. Structures of AHPN (**1**), 5-Cl-AHPN (**2**), 5-Me-AHPN (**3**), AHPC (**4**), 3-Cl-AHPC (**5**), 3-A-AHPC (**6**), trans-RA (**7**), TTNN (**8**), 5-Me-TTNN (**9**), and TTNC (**10**).

inducing the cell-cycle arrest and initiating the apoptosis of MCF-7 breast cancer and other cancer cell lines.^{3,4} Further research led to our identification of (*E*)-4-[3'-(1-adamantyl)-4'-hydroxyphenyl]-3-chlorocinnamic acid (3-Cl-AHPC, **5**)⁵ that retained these functions but not that exhibited by classical retinoids, namely the transcriptional activation of the retinoic

acid nuclear receptor (RAR) subtypes to induce the transcription of genes regulated by *trans*-retinoic acid (*trans*-RA, **7**) and its synthetic retinoid analogues.^{5–8} By inducing apoptosis of leukemia cells obtained from AML patients,⁵ **5** may have potential as a therapeutic agent for treating acute myeloid leukemia (AML). It also has the ability to induce apoptosis of cells from a variety of human cancer cell lines, including those derived from breast, lung, and prostate cancers.⁹ Moreover, apoptosis induced by **1** and **5** was found to be independent of the sensitivity of the cancer cell line to growth regulation by *trans*-RA or its p53 status,^{3,4} either of which is therapeutically advantageous because during cancer progression the ability of the *trans*-RA–RAR α complex to regulate proliferation or induce differentiation through induction of expression of the tumor suppressor gene RAR β is lost^{10,11} and the tumor suppressor gene p53 becomes dysfunctional or lost in about 50% of tumors.^{12,13}

Recently, we identified the first synthetic small-molecule ligands, 3-Cl-AHPC (**5**) and several analogues, for the nuclear receptor small heterodimer partner (SHP; NROB2),¹⁴ which hitherto had only a putative ligand-binding domain and was classified as an orphan receptor. SHP is an atypical member of the steroid/thyroid hormone nuclear receptor family of transcription factors because it lacks the amino terminal sequence (AB), canonical DNA-binding domain (C), and hinge region (D) that are typical of other nuclear receptors and predominately functions as a transcriptional repressor through the binding of one of its three NR box motifs (LXXLL) to the activation function 2 (AF-2) site in the ligand-binding domain of its dimeric nuclear receptor partner. SHP has been found to bind such nuclear receptors as the androgen, aryl hydrocarbon receptor nuclear translocator, constitutive activated, estrogen, farnesoid, glucorticoid, liver X, pregnane X, peroxisome proliferator-activated, retinoic acid, retinoid X, thyroid hormone, TR3/nur77/NGFB-I, and vitamin D receptors.^{15–21} SHP modulates gene transactivation or suppression induced by its heterodimeric partner by recruiting histone deacetylases 1, 3, or 6, G9a histone 3 K9 methyltransferase, and other members of the Sin3a–Swi/Snf repressor complex.¹⁷

Tumor growth can be inhibited directly by inducing cancer cell death or indirectly by inhibiting tumor neovascularization (angiogenesis), a process that provides a conduit for delivery of nutrients to and removal of metabolic byproducts from the tumor.²² Tumor vasculature also provides a route for cancer cells to escape from the tumor and move to secondary metastatic sites.²³ For these reasons, we explored the abilities of 3-Cl-AHPC (**5**) and its analogues to function as anticancer and antiangiogenic agents. We also undertook an analogue generation program to determine the pharmacophoric elements necessary to confer apoptotic activity to **5**. Here, we report the effects of **5** and several analogues on the proliferation and functions of human microvascular endothelial (HMVE) cells and the impact that replacing the carboxylic acid group of **5** with other hydrogen-bond acceptors or isosteric-like groups has on cancer cell growth inhibition and induction of apoptosis.

Results and Discussion

Chemistry. Analogue Design. As a consequence of reports that therapeutic retinoids and RAR ligands such as *trans*-RA (**7**) and 9-*cis*-RA can cause adverse effects in cancer patients,^{24,25} a major facet of our design strategy has been introducing groups and scaffold modifications onto the AHPN scaffold that reduced interaction with the RAR subtypes. This strategy was first accomplished for the design of AHPC (**4**) by comparing the activities of members of our retinoid library in assays for retinoid

Table 1. Classical Retinoid Assays Used To Compare Activities of Conformationally Restricted Retinoids with Those of *trans*-Retinoic Acid^a

retinoid	IC ₅₀ value (nM)		ID ₅₀ value (nmol)
	TOC ^b	F9 ^c	ODC ^d
<i>trans</i> -RA (7)	0.01	0.1	0.19
TTNN (8)	0.007	1.0	2.0
TTNC (10)	0.32	0.3	7.5
AHPN (1)	nd ^e	nd	3.1
5-Me-TTNN (9)	0.08	3.0	66

^a For overview of these assays see Sporn and Roberts (1984). ^b TOC assay, concentration required to reverse keratinization in 50% of vitamin A-deficient hamster tracheas in organ culture after 10 days as determined by analysis of stained cross-sections for the absence of keratin and keratohyaline granules. ^c F9 assay, concentration required to induce terminal differentiation in 50% of F9 murine embryonic teratocarcinoma cells in culture after 3 days as measured by secreted plasminogen activator activity. ^d ODC assay, topical dose of retinoid preapplied to mouse dorsal epidermis at 1 h before TPA leading to 50% inhibition in level of ornithine decarboxylase induced by TPA (7.5 nmol) at 4.5 h after TPA application as measured by the release of labeled CO₂ from [¹⁴C]ornithine by epidermal homogenates. TPA, 12-*O*-tetradecanoylphorbol-13-acetate. ^e nd, not determined.

activity with those of the retinoid TTNN (**8**)²⁶ from which AHPN (**1**) was originally derived.² These assays, which historically have been widely used to assess retinoic acid-like activity, were (i) induction of keratin granule formation in vitamin-A-deficient hamster trachea in organ culture (TOC assay), which was developed by Sporn and co-workers;²⁷ (ii) induction of differentiation in F9 embryonic teratocarcinoma cells (F9 assay);²⁸ and (iii) inhibition of the induction of the proliferative enzyme ornithine decarboxylase in mouse epidermis by the tumor promoter 12-*O*-tetradecanoylphorbol-13-acetate (TPA), which was developed by Verma and Boutwell (ODC assay).²⁹ These assays have been reviewed by Sporn and Roberts.³⁰ On the basis of its lower activities in the TOC and ODC assays, the cinnamic acid analogue (TTNC, **10**)³¹ of TTNN (**8**) was deemed to have less retinoid activity (Table 1). Similarly, the 3'-(1-adamantyl)-4'-hydroxyphenyl ring of **1** conferred lower retinoid activity than the 5,6,7,8-tetrahydro-5,5,8,8-tetramethyl-2-naphthalenyl ring of **8**²⁶ did in the ODC assay³² (Table 1), just as it was subsequently found by Shroot and co-workers to have lower activity in the RAR transcriptional activation assay.¹ Therefore, the two ring systems, 3-(1-adamantyl)-4-hydroxyphenyl and (*E*)-cinnamic acid, were joined at their 1- and 4-ring positions, respectively, to produce AHPC (**4**).

AHPC (**4**) effectively induced cancer cell apoptosis and exhibited lower activities in the TOC, F9, and ODC assays than AHPN; however, we observed that mice injected intravenously with AHPC displayed symptoms of retinoid-like toxicity. The structure of **4** was later reported as ST1926, which was found to have antileukemic activity.³³ Recently, **4** was also found to transactivate the RARs α , β , and γ on a DR5-*tk*-CAT reporter construct in transfected COS-7 cells.³⁴ Its half-maximal activation concentrations (AC₅₀s) were 8-, 2.8-, and 4.7-fold higher, respectively, than those of *trans*-RA (**7**), thereby supporting our design strategy.

As Table 1 indicates, introduction of a substituent at the 5-position of the naphthalene ring in TTNN (**8**), which is ortho to the diaryl bond, reduced the retinoid activity of 5-Me-TTNN (**9**) in the TOC, F9, and ODC assays. By adapting this substitution strategy, namely introducing a chloro group adjacent to the diaryl bond of AHPN (**1**) and AHPC (**4**), we achieved a further reduction in RAR interaction by energetically hindering the diaryl rings of 5-Cl-AHPN (**2**)³⁵ and 3-Cl-AHPC (**5**)⁵ from assuming a small dihedral angle on binding to the RARs.⁶

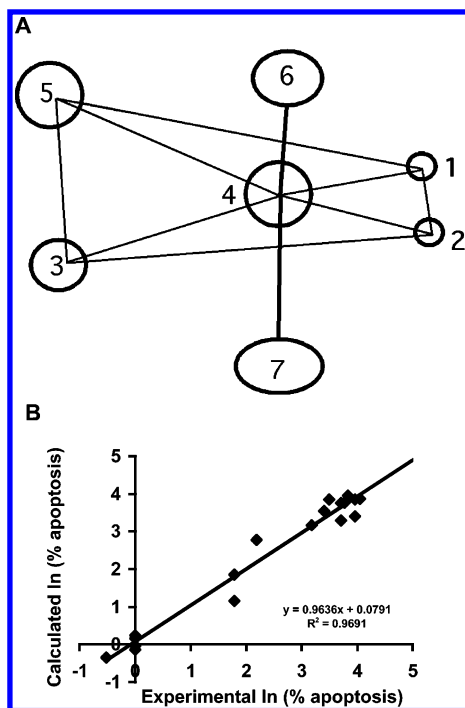
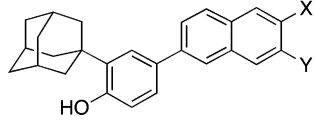
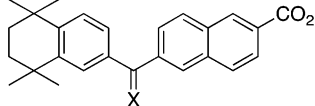


Figure 2. Pharmacophoric model showing essential components of apoptosis-inducing activity used for the design of 3-Cl-AHPC and its analogues. (A) Three-dimensional seven-point pharmacophore descriptive of common elements in compounds in an AHPN analogue training set of which 44% were active at inducing MDA-MB-231 breast cancer cell apoptosis at 1.0 μ M after a 96-h treatment. Components 1 and 2, hydrogen-bond acceptor; 3, hydrogen-bond donor/acceptor; 4, hydrophobic ring; 5, hydrophobic group; 6, sterically accessible hydrophobic region; and 7, sterically accessible polar-permissible region. Interpoint distances (\AA) \pm SD: $\Delta_{(1-2)}$, 2.1 ± 0.01 ; $\Delta_{(1-3)}$, 12.5 ± 0.1 ; $\Delta_{(1-4)}$, 5.9 ± 0.1 ; $\Delta_{(1-5)}$, 12.4 ± 1.2 ; $\Delta_{(2-3)}$, 12.5 ± 0.2 ; $\Delta_{(2-4)}$, 5.7 ± 0.2 ; $\Delta_{(3-5)}$, 4.0 ± 0.1 ; $\Delta_{(4-5)}$, 7.5 ± 0.1 ; $\Delta_{(4-6)} \geq 2.3$. (B) Comparative molecular similarity index analysis on 19 analogues using the overlap rule/pharmacophore defined in (A) for prediction of induction of apoptosis of MDA-MB-231 breast cancer cells after treatment for 96 h at 1.0 μ M by comparing natural logs of experimental and calculated values. Predictive $R^2 = 0.78$; uncross-validated $R^2 \pm \text{SE} = 0.95 \pm 0.45$.

According to molecular dynamics calculations on **2**, the increased dihedral angle for the 1',4-diaryl bond caused the adamantyl group to interfere with the local dynamics of RAR γ helix H12 to prevent the formation of the AF-2 site with helices H3 and H4 to which coactivator proteins bind to recruit the transcriptional complex necessary for retinoid-induced gene transcription.

We recently undertook quantitative structure–activity relationship (SAR) studies to identify the core recognition elements on 55 analogues of AHPN (**1**) and AHPC (**4**) that were necessary to induce the apoptosis of MDA-MB-231 breast cancer cells after treatment at 1.0 μ M for 96 h. The ‘overlap rule’ was used to align the training set in SYBYL QSAR, and the comparative molecular similarity index analysis (CoMSIA) electrostatic, hydrophobic, and steric fields were computed on a grid surrounding the overlapped ligands. The resulting CoMSIA analysis for apoptosis induction in MDA-MB-231 breast cancer cells [$\ln(\% \text{ apoptosis})$] resulted in a predictive R^2 of 0.78 and an un-cross-validated R^2 of 0.95 with a standard error of 0.45. This seven-point descriptive model is illustrated in Figure 2A. Key polar points include two adjacent hydrogen-acceptor groups 1 and 2 and a hydrogen-donor/acceptor group 3. The predictivity of this initial model was sufficient to score apoptosis induced by analogues similar in character to those in the training set. For example, if 3-Cl-AHPC (**5**) and (*E*)-3-[5-[3'-(1-adamantyl)-

Table 2. Comparison of Effects of 3-Cl-AHPC (**5**) and Its Analogues on HMVE Cell Proliferation after 96 h of Treatment Compared to *trans*-Retinoic Acid (**7**) and Synthetic RAR γ -selective Analogues **13** and **14**

compound	IC ₅₀ (μ M) ^a	inhibition (%) at 0.5 μ M ^b
AHPN (1)	0.3	70
5-Cl-AHPN (2)	0.5	45
AHPC (4)	0.1	90
3-Cl-AHPC (5)	0.3	60
<i>trans</i> -RA (7)	>0.5 ^c	10
		
AHPN-3-CO ₂ H (11) X = H, Y = CO ₂ H	>0.5 ^c	15
AHPN-2-OH (12) X = OH, Y = H	>0.5 ^c	15
		
13 X = NHOH	>0.5 ^c	30
14 X = (SCH ₂) ₂	>0.5 ^c	15

^a Concentration inhibiting proliferation by 50%. ^b Relative to vehicle alone control. ^c Highest concentration evaluated.

4'-hydroxyphenyl]-2-thienyl]propenoic acid were left out of the training set and the CoMSIA model were used to predict their ability at 1.0 μ M to induce MDA-MB-231 apoptosis, the predicted versus experimental results were: 92% versus 43% for **5** and 0.8% versus 1% for the thienylpropenoic acid (Figure 2B). Thus, while not quantitative, even at this level the CoMSIA model was able to make order of magnitude predictions, underscoring the reasonableness of the model and the underlying pharmacophore. In the study reported here, we focus on identifying the character of the hydrogen-acceptor group(s) 1 and/or 2 required for induction of apoptosis.

Replacement of the carboxylic acid group of 3-Cl-AHPC (**5**) by isosteric and other groups having a similar pattern of polar atoms that function as hydrogen-bond acceptors was explored to determine whether pharmacologic properties could be improved with retention of apoptotic activity. Our earlier studies indicated that shifting the position of the carboxylate group relative to the phenolic hydroxyl was not successful. No apoptosis of *trans*-RA-resistant HL-60R leukemia cells³⁶ was observed after 24-h treatment with 1.0 μ M 6-[3'-(1-adamantyl)-4'-hydroxyphenyl]-3-naphthalenecarboxylic acid (**11** in Table 2), compared to 98% apoptosis with 1.0 μ M AHPN (**1**). The 96-h treatment of retinoid-resistant MDA-MB-231 breast cancer cells with 2.0 μ M 5-[3'-(1-adamantyl)-4'-hydroxyphenyl]-1-naphthalenecarboxylic acid produced only 4% apoptosis, compared to 46% apoptosis of MDA-MB-231 cells induced by 1.0 μ M **1**. Replacement of the 2-carboxylate group with phenolic hydroxyl, carboxamide, and *N*-ethyl sulfonamide groups was similarly unsuccessful. Only 15% inhibition of primary human microvascular endothelial (HMVE) cell growth resulted on treatment with 1.0 μ M 6-[3'-(1-adamantyl)-4'-hydroxyphenyl]-2-naphthol (**12**). The carboxamide derivative of 5-Me-AHPN (**3**) at 1.0 μ M or 5.0 μ M was essentially inactive at inducing retinoid-resistant KG-1 AML cell apoptosis at 48 h (3% and 5%, respectively, compared to 2% apoptosis in the vehicle-treated control) although **3** at 1.0 μ M and 5.0 μ M induced 51% and 73% apoptosis, respectively. After 48 h, KG-1 AML cell growth inhibition by the carboxamide derivative of **3** at 5.0 μ M

was 3% compared to 2% in the control and 96% in 5.0 μM 3-treated cells. Similar results were obtained after 72 h of treatment. Evidently, KG-1 cells were unable to cleave a primary amide to the active carboxylate. Apoptosis induced in MDA-MB-231 cells after a 96-h treatment with the 2-(*N*-ethyl sulfonamide) analogue of **1** at 2.0 μM was only 2%, although growth inhibition was 30%.

Because shifting the 2-carboxyl group of AHPN (**1**) to the 3-position and replacing the 2-carboxyl group by a hydroxyl group (**11** and **12** in Table 2) were unpromising, other modifications were investigated using 3-Cl-AHPC (**5**) as the scaffold. The tetrazole and thiazolidinedione termini were investigated using analogues **24**, **31**, **39**, and **43**. These termini were reported to reduce retinoid activity by the Dawson³² and Shudo^{37,38} groups, respectively. The ability of nitriles (C=O bioisostere)³⁹ and hydroxamates to function as hydrogen-bond acceptors led to the design of **45** and **48**, respectively. The boronic acid and phosphonic acid monoethyl ester analogues (**57** and **63**, respectively) were also investigated. In the latter case, the monoester rather than the free acid was prepared to improve membrane permeability.

On the basis of our finding that commonly used carboxylate replacements (OH and CONH₂) resulted in loss of apoptotic activity, we hypothesized that the carboxylate group of 3-Cl-AHPC (**5**) was crucial for bioactivity. Retinoid carboxylates are known to form strong salt bridges with the side-chain guanidinium groups of arginines in the ligand-binding pockets of RARs and RXRs. For example, the crystallographic structure of trans-RA (**7**) bound to the RAR γ ligand-binding domain (PDB 2LBD) reveals a strong salt bridge between the carboxylate of **7** and the guanidinium group of Arg-278 located at the C-terminus of helix 5.^{40,41} We further hypothesized that a putative arginine in the receptor protein for **5**⁴² could interact with the carboxylate of **5**. If this were correct, an analogue bearing a terminal 2-oxoaldehyde could undergo the Maillard reaction with the arginine guanidinium group or at least hydrogen-bond with this group. Methyl glyoxal and α -diones undergo the Maillard reaction with the arginine guanidinium group to form pyrimidines.^{43–45} 2-Oxoaldehyde **60** was designed to test this hypothesis. The structures of these isosteric carboxylate analogues are shown in Table 3.

Synthesis. Routes to the 3-Cl-AHPC (**5**) analogues are shown in Schemes 1 and 2. Like **5**, these analogues are characterized by a tetrasubstituted 1,1'-biphenyl core that was introduced by a Suzuki–Miyaura diaryl coupling reaction⁴⁶ between the arylboronic acid **16** and a 4-substituted 2-chlorophenyl triflate (**21**, **28**, **34**, **40**, or **50**) using tetrakis(triphenylphosphine)-palladium as the catalyst generally in the presence of LiCl and an aqueous base in refluxing dimethoxyethane (Schemes 1 and 2). Coupling yields ranged from 51% to 91%. Intermediate **16**⁶ was prepared in three steps (74% overall yield), namely (i) Friedel–Crafts monoalkylation of 4-bromophenol (**15**) with 1-adamantanol catalyzed by methanesulfonic acid or concd sulfuric acid, which gave comparable yields of 2-(1-adamantyl)-4-bromophenol and no detectable diadamantylation product; (ii) protection of the phenolic hydroxyl group of the adamantylation product as the benzyl ether; and (iii) low-temperature (–78 °C) lithium–halogen exchange of resultant 3-(1-adamantyl)-4-benzyloxybromobenzene using *n*-butyllithium, conversion of the aryllithium to the arylboronate ester by treatment with tri(isopropyl) borate, and acid hydrolysis during workup.

4-Hydroxyl-3-chlorobenzaldehyde (**17**) was used to generate four of the triflate intermediates (**21**, **28**, **34**, and **40**) as shown in Scheme 1. In the case of the tetrazole-terminated targets **24**

and **31** and the thiazolidinedione-terminated target **39**, the hydroxyl group of **17** was protected as the benzyl ether so that benzaldehyde **18** could be elongated to cinnamionitrile **19** and ethyl cinnamate **32** by olefination chemistry or be derivatized to the hydroxylimine **25** for dehydration to produce benzonitrile **26**. The *E* isomer predominated in the olefination products **19** and **32** according to their ¹H NMR spectra, which indicated about 5% of the *Z* isomer at most. The unwanted isomer was readily removed by chromatography. Low-temperature (–78 °C) cleavage of the benzyl ether protecting groups from **19**, **26**, and **32** using boron tribromide afforded phenols **20**, **27**, and **33**. These phenols and **17** were converted to their respective triflates **21**, **28**, **34**, and **40** using triflic anhydride and pyridine in dichloromethane. Diaryl coupling of the triflates with **16** introduced the substituted 1,1'-biphenyl scaffolds of intermediates **22**, **29**, **35**, and **41**, respectively.

After removal of the benzyl protecting groups from **22** and **29**, the nitrile groups of their parent phenols **23** and **30** were allowed to undergo cycloaddition with trimethylsilyl azide in the presence of di(*n*-butyl)tin oxide⁴⁷ to introduce the 5-substituted tetrazole termini of targets **24** and **31**, respectively. The ethyl cinnamate, intermediate **35**,³⁵ was converted by hydride reduction followed by Swern oxidation⁴⁸ to (*E*)-cinnamaldehyde **37**, which was subjected to condensation/elimination with 2,4-thiazolidinedione to afford the 5-cinnamylidene-2,4-thiazolidinedione **38**. The substituted benzaldehyde, intermediate **41**, was similarly transformed to the 5-benzylidene-2,4-thiazolidinedione **42**. Thiazolidinedione formation produced both double-bond isomers. Their ¹H NMR spectra indicated that the *Z*-double bond isomers **38** and **42** predominated as demonstrated by the downfield positions (0.4 ppm) of their vinylic protons trans to the sulfur atom (H–C=C–S) compared to those that were cis. Chromatographic purification and debenzoylation of **38** and **42** afforded the 5-cinnamylidene- and 5-benzylidene-2,4-thiazolidinedione targets **39** and **43**, respectively. Knoevenagel condensation of benzaldehyde **41** with malononitrile⁴⁹ and debenzoylation produced the 2-benzylidenepropanedinitrile **45**. However, if **17** were first converted to the 2-(3'-chloro-4'-hydroxybenzylidene)propanedinitrile and then treated with triflic anhydride, the triflate ester was not obtained.

Syntheses of hydroxamic acid **48**, boronic acid **57**, 2-oxoaldehyde **60**, and monoethyl phosphonate **63** are outlined in Scheme 2. Cinnamyl ester **35** from Scheme 1 was hydrolyzed to cinnamic acid **46**,³⁵ which was converted to the activated ester by treatment with diisopropylcarbodiimide and 4-dimethylaminopyridine. Reaction of this ester with the tetrahydropyranil ether of hydroxylamine⁵⁰ produced the protected hydroxamic acid **47**. Concomitant low-temperature cleavage of the benzyl and tetrahydropyranil protecting groups with boron tribromide afforded the hydroxamic acid target **48**. Reaction of the activated ester of 3-Cl-AHPC (**5**) with hydroxylamine failed to produce **48** in the presence of the unprotected phenolic group.

Construction of the 2-arylethenylboronic acid **57** was accomplished in eight steps from 2-chloro-4-nitrophenol (**49**). Because aryl bromides and triflates typically undergo coupling with boronic acids with equal efficiency and the ortho chloro group in **49** was expected to hinder coupling by the aryl triflate, the bromo group was masked as a nitro group in triflate **50** to accomplish coupling with **16**. The nitro group in the coupled product, **51**, was then transformed to the bromo group by reduction to the amine and diazotization under hydrophobic conditions using *tert*-butyl nitrite in the presence of cupric bromide.⁵¹ Aryl bromide **53** underwent Sonagashira coupling with trimethylsilylacetylene⁵² to give the protected phenylacety-

Table 3. Effects of 3-Cl-AHPC (**5**) and Analogues on Leukemia Cell Apoptosis and Leukemia and Cancer Cell Proliferation

compound	R	KG-1 AML apoptosis (%) ^a		KG-1 AML ^b	growth inhibition IC ₅₀ value (μM) (% inhibition at 1.0 μM)		
		1.0 μM	5.0 μM		MDA-MB-231 breast ^c	H292 lung ^c	DU-145 prostate ^c
5		35	55	0.30 (44)	1.8 (32)	0.4 (79)	0.5 (76)
24		10	12	13 ^d (0)	21 (0)	16 (3)	14 (0)
31		2	2	>5 ^e (13)	71 (0)	14 (3)	52 (0)
39		2	2	>5 ^f (0)	24 (0)	23 (2)	15 (0)
43		8	10	14 ^d (28)	18 (0)	3.6 (17)	3.7 (17)
45		0	3	>5 ^e (0)	>10 ^e (0)	>10 ^e (0)	>10 ^e (4)
48		0	4	>5 ^e (0)	6.3 ^d (4)	9.0 ^d (6)	3.5 (7)
57		4	4	>5 ^e (0)	19 ^f (3)	7.2 (0)	7.0 (2)
60		5	6	10 ^d (11)	14 (0)	7.0 (7)	7.8 (0)
63		0	0	>5 ^e (0)	>5.0 ^e (3)	>5.0 ^e (2)	>5.0 ^e (3)

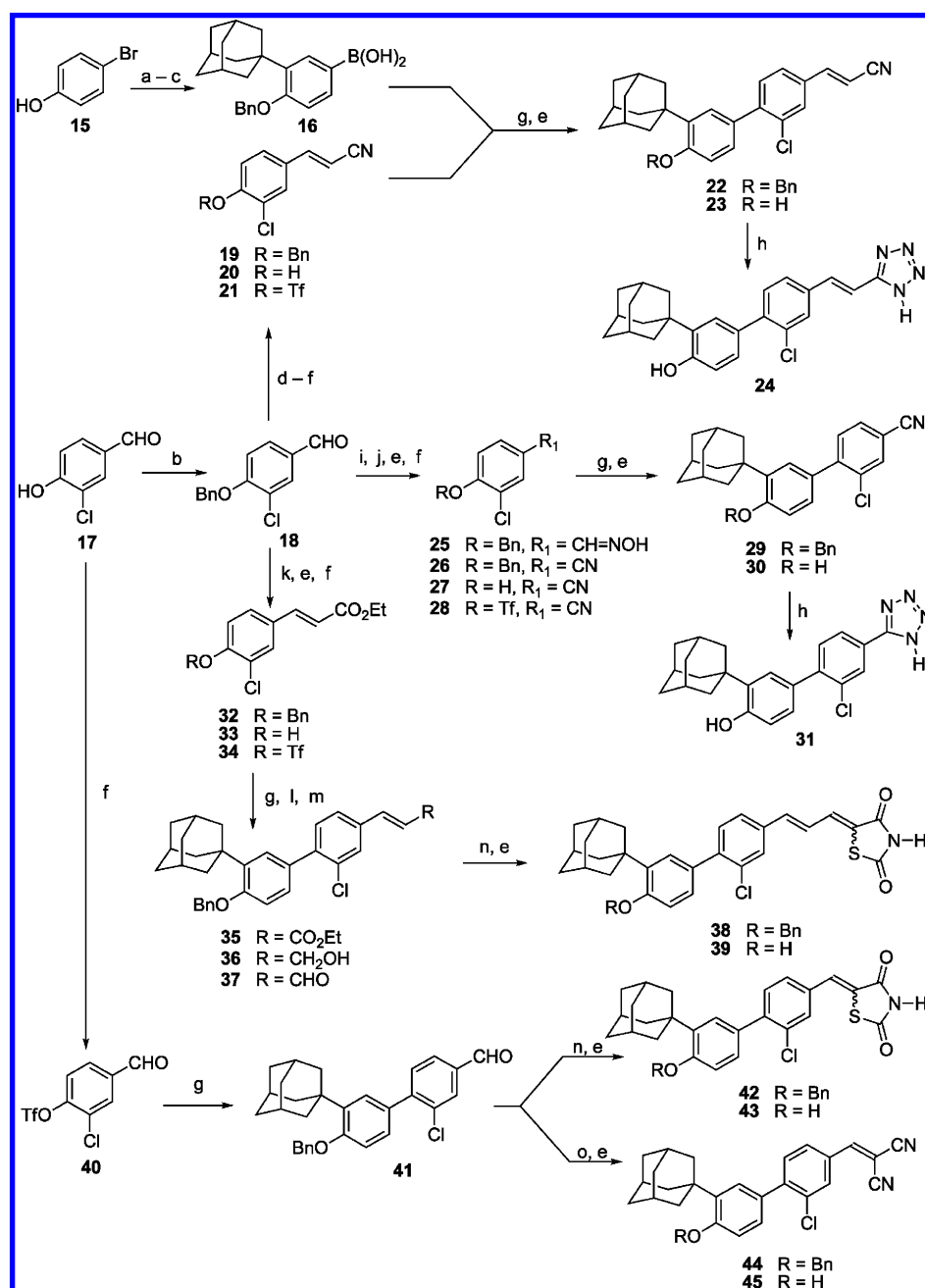
^a Apoptosis after 48 h of treatment. ^b Inhibition of proliferation relative to vehicle-alone control after 48 h of treatment for KG-1 leukemia cells. ^c Inhibition of proliferation relative to vehicle-alone control after 72 h for solid tumor cell lines, with one media ± compound change after 48 h. At 5.0 μM, inhibition of KG-1 AML growth was as follows: **5**, 67%; **24**, 31%; **31**, 21%; **39**, 2%; **43**, 41%; **45**, 0%; **48**, 0%; **57**, 0%; **60**, 38%; **63**, 0%. ^d Extrapolated value; highest concentration evaluated was 5.0 μM. ^e Low activity at highest concentration evaluated (5.0 μM or 10 μM) did not permit extrapolation. ^f Extrapolated value; highest concentration evaluated was 10 μM.

lene **54**. Desilylation of **54** with tetra(*n*-butyl)ammonium fluoride⁵² provided phenylacetylene **55**. Benzodioxaborole **56** was prepared by the cis-hydroboration of **55** with catecholborane.⁵³ Treatment of **56** with boron tribromide (−78 °C) cleaved both benzodioxo and benzyl protecting groups to produce the (*E*)-2-phenylethenyl boronic acid **57**.

To prepare the 2-oxoketoaldehyde **60**, we introduced the (*E*)-2-oxopropylidene group of **58** by olefination of benzaldehyde **41**⁶ with the ylid derived from (2-oxopropyl)triphenylphosphonium bromide.⁵⁴ The aldehyde group of **59** was obtained by selenous acid oxidation⁵⁵ of the methyl group of **58**. Debenzylation of **59** afforded **60**. Horner–Emmons–Wadsworth olefination of **41** using the anion of tetraethyl methylenediphosphonate⁵⁶ produced diethyl phosphonate **61**, which on acid hydrolysis⁵⁷ and debenzoylation with boron tribromide produced the monoethyl phosphonate **63**.

Biological Activity. Of the compounds shown in Table 3, only 3-Cl-AHPC (**5**) efficiently induced KG-1 cell apoptosis after a 48-h treatment at 1.0 μM (30%) or 5.0 μM (55%). Its

inhibition of cell growth was comparable (44% and 67%, respectively). After 96 h of treatment with 1.0 μM **5**, apoptosis rose to 66% compared to 7% in the Me₂SO-alone control. Evidently, the region of the target protein with which the carboxylate group of **5** interacts to mediate its apoptotic effects is sufficiently constrained to prevent the other hydrogen-acceptor groups in the analogues shown in Table 3 from efficient interaction. However, similar constraints did not appear to impact inhibition of proliferation as potently. Thus, tetrazoles **24** and **31** and thiazolidinedione **43** were modest inhibitors of KG-1 cell proliferation as measured by cell counting but induced minimal apoptosis (2%–10% compared to 2%–3% in the control). On the basis of its efficient overlap with **5** and structural similarity, we had predicted that tetrazole **24** would have significant antiproliferative and apoptotic activities and that the longer thiazolidine **39** would lack such activities. However, both proved to be inactive in the apoptosis induction assays, and **39** lacked antiproliferative activity. 2-Oxoaldehyde **60** was also unable to induce apoptosis but did show weak growth inhibition

Scheme 1^a

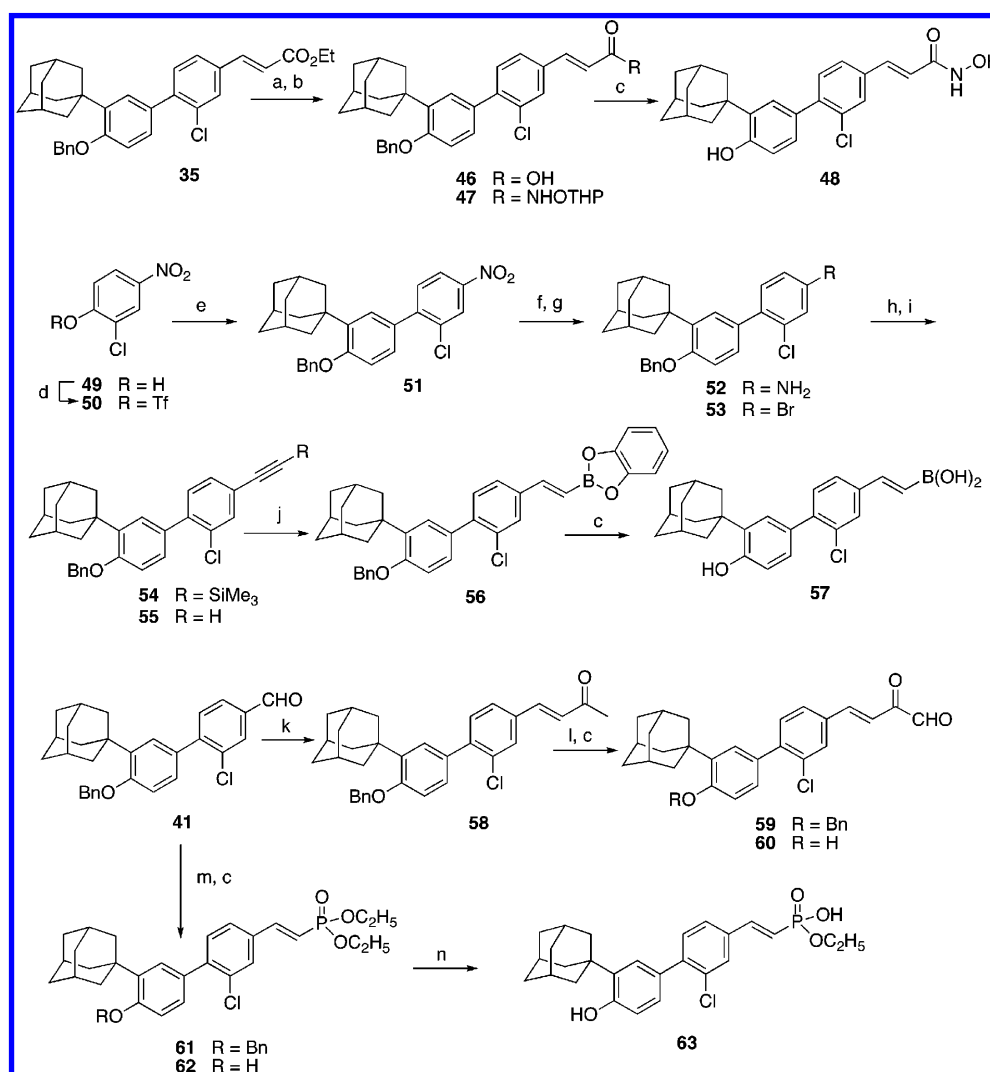
^a Reagents and conditions: (a) 1-AdOH, concd H₂SO₄, CH₂Cl₂. (b) PhCH₂Br, K₂CO₃, acetone, reflux. (c) *n*-BuLi, -78 °C; B(Oi-Pr)₃, -78 °C to room temperature; dil. HCl. (d) [(EtO)₂P(O)CH₂CN, KN(TMS)₂, THF, -78 °C], -78 °C to room temperature. (e) BBr₃, CH₂Cl₂, -78 °C; H₃O⁺. (f) Tf₂O, pyridine, CH₂Cl₂, 0 °C to room temperature. (g) **16**, Pd(PPh₃)₄, 2 M Na₂CO₃, LiCl, DME, reflux. (h) Me₃SiN₃, (*n*-Bu)₂SnO, PhMe, 90° to 95 °C. (i) NH₂OH·HCl, MeOH, pyridine, 50 °C. (j) MeSO₂Cl, PhMe, pyridine. (k) [(EtO)₂P(O)CH₂CO₂Et, KN(TMS)₂, THF, -78 °C], -78 °C to room temperature. (l) DIBAL, CH₂Cl₂, -78 °C; dil. HCl. (m) (COCl)₂, Me₂SO, NEt₃. (n) 2,4-Thiazolidinedione, HOAc, NHET₂, PhMe, 50° to 60 °C. (o) CH₂(CN)₂, DMF, reflux.

(38% at 5.0 μM). Recently, we demonstrated that 3-A-AHPC (**6**) antagonized **5**-induced apoptosis but retained antiproliferative activity.⁶

3-Cl-AHPC (**5**) and its analogues were also assessed for their abilities to inhibit the proliferation of retinoid-resistant MDA-MB-231 breast, H292 lung, and DU-145 prostate cancer cells grown in the presence of 10% fetal bovine serum. Dose-response curves are shown in Figure 3. On the basis of their IC₅₀ values (Table 3), H292 and DU-145 cells were generally more sensitive to inhibition under these growth conditions than MDA-MB-231 cells (Figure 3). The most potent inhibitor in the series was **5**. Thiazolidinedione **43** displayed modest growth inhibitory activity against the lung and prostate cancer cell lines

(IC₅₀ = 3.6 and 3.7 μM, respectively). Hydroxamic acid **48** displayed similar activity against prostate cancer cells (IC₅₀ = 3.5 μM) and had an IC₅₀ of about 6.3 μM (extrapolated value) against breast cancer cells. The other analogues were less active.

Most of the AHPN analogues in the original training set for apoptosis induction had a carboxyl group at the 2-position of the naphthalene ring. Modifying this group had a deleterious impact on apoptosis induction but not on inhibition of proliferation (Table 3). We next addressed the impact on KG-1 cell growth of variations in the position and character of the polar hydrogen-bond acceptor region (descriptive points 1 and 2 in Figure 2A) in an attempt to understand the biological data in terms of fundamental changes in the polar region. Thus, a

Scheme 2^a

^a Reagents and conditions: (a) LiOH·H₂O, THF, H₂O; dil. HCl. (b) H₂NOTHP, DIC, DMAP, CHCl₃, 0 °C to room temperature. (c) BBr₃, CH₂Cl₂, −78 °C; H₃O⁺. (d) Tf₂O, pyridine, CH₂Cl₂, 0 °C to room temperature. (e) **16**, Pd(PPh₃)₄, aq K₃PO₄, DME, reflux. (f) SnCl₂·2 H₂O, EtOH, reflux. (g) CuBr₂, *t*-BuNO₂, MeCN, 0 °C to room temperature. (h) Pd(PPh₃)₃, CuI, Et₃N, Me₃Si-acetylene, reflux. (i) (*n*-Bu)₄NF, THF. (j) Catecholborane, THF, reflux. (k) MeCOCH₂P(Ph)₃Br, 1,5,7-triazabicyclo[4.4.0]dec-5-ene, THF, room temperature to 70 °C. (l) H₂SeO₃, dioxane/H₂O (10:1). (m) Tetraethyl methylene-diphosphonate, 50% aq NaOH, CH₂Cl₂. (n) 20% aq HCl, reflux.

fragment QSAR model was constructed using the isosteric polar/hydrogen-bond acceptor replacements shown in Table 3 for the carboxyl group of 3-Cl-AHPC (**5**). While the number of analogues included in this portion of the SAR study was limited, a predictive fragment QSAR, $\ln(\text{IC}_{50} \text{ KG-1}) = -2.65 + 0.121\text{POLAR_V} + 0.062 \text{p}K_a$ (raw), having an R^2 of 0.76 and a standard error of 0.78, using two independent variables could be developed and related to the $\ln(\text{IC}_{50})$ values.⁵⁸ Polar volume (POLAR_V) and calculated (raw) $\text{p}K_a$ were the most important features influencing KG-1 growth inhibition. For the solid tumor cell lines, modestly predictive QSAR models ($R^2 = 0.5\text{--}0.8$) were developed using the three properties of the longest length of the fragment (L), minimum in computed electrostatic potential on the van der Waals surface of the fragments (MINIM_PS) and polar volume. In Figure 4 is illustrated the quality of the three-parameter QSAR model for MDA-MB-231 breast cancer cell growth inhibition IC_{50} values in terms of these properties. The resultant analysis had an R^2 of 0.75 and a standard error of 0.6. The QSAR equation $\ln(\text{IC}_{50} \text{ MBA-MB-231}) = 4.14 - 0.30L + 14.9\text{MINIM_PS} + 0.10\text{POLAR_V}$ with the 'weights' of the elements revealing their 'relative contributions'. Analogously, analysis of the results on the other cell lines yielded

similar equations: $\ln(\text{IC}_{50} \text{ H292}) = 3.33 + 0.28L + 11.78\text{MINIM_PS} + 0.090\text{POLAR_V}$ with an R^2 of 0.44 and a standard error of 1.1 and $\ln(\text{IC}_{50} \text{ DU-145}) = 3.87 - 0.073L + 19.3\text{MINIM_PS} + 0.10\text{POLAR_V}$ with an R^2 of 0.54 and a standard error of 1.0. While the predictive R^2 values are only modest, the analyses do indicate that both the amount of polar atom (group) exposure and size are correlated with antiproliferative activity, whereas the other computed properties are not explanatory variables. Therefore, the analyses provide a preliminary indication of molecular design features coupled to growth inhibitory activity variations.

The NR4A1 nuclear receptor protein was found to interact in the cytoplasm with the mitochondrial protein Bcl-2 to induce cancer cell apoptosis.⁵⁹ The translocation of NR4A1 from nucleus to cytoplasm was observed to occur in several cancer cell lines after their transfer to media lacking serum and treatment with an analogue of AHPN (**1**). Once in the cytoplasm, NR4A1 was able to induce a proapoptotic conformational change in antiapoptotic Bcl-2 that led to mitochondrial cytochrome c release followed by apoptosis. Therefore, we attempted to correlate the sensitivity of MDA-MB-231 breast, H292 lung, and DU-145 prostate cancer cells to apoptosis induction by 3-Cl-

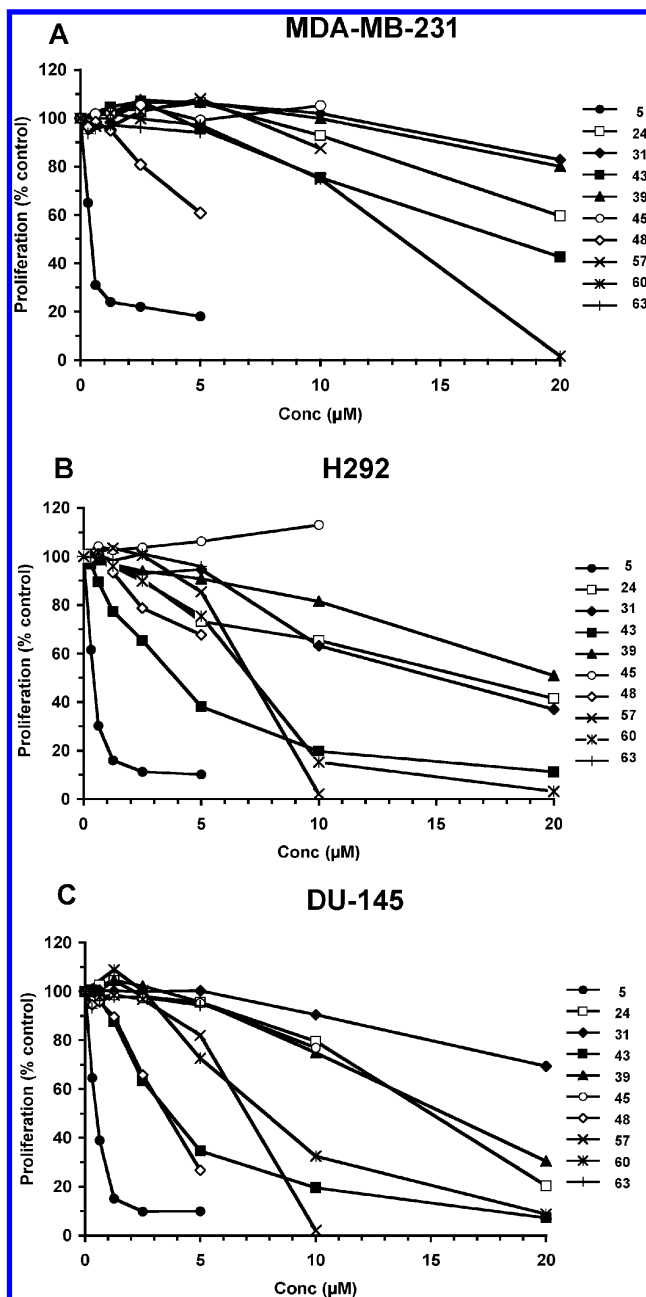


Figure 3. Effects of 3-Cl-AHPC (**5**) and analogues **24**, **31**, **39**, **43**, **45**, **48**, **57**, **60**, and **63** on proliferation of trans-retinoic acid-refractory cancer cell lines after treatment for 72 h as described in the Experimental Section. (A) MDA-MB-231 breast cancer; (B) H292 lung cancer; and (C) DU-145 prostate cancer. Results shown are the averages of three replicates. Standard errors were below 10%.

AHPC (**5**) with their levels of NR4A1 (human TR3) protein expression. In lysates obtained from these cancer cell lines that had been both grown and treated with 1.0 μM **5** in media containing 10% fetal bovine serum we were not able to detect NR4A1 protein by Western blotting (data not shown). These results suggest that serum constituents could influence NR4A1 expression.

After Zhang et al.⁶⁰ found evidence to suggest that AHPN (**1**) modulated enzyme activity on the basis of (i) its rapid induction of cell-cycle arrest and apoptosis; (ii) its lack of a requirement for gene transcription or protein synthesis as evidenced by resistance to actinomycin D or cycloheximide treatment, respectively, and (iii) its ability to inhibit the phosphatidylinositol-3-kinase (PI3-K)/Akt pathway, we hy-

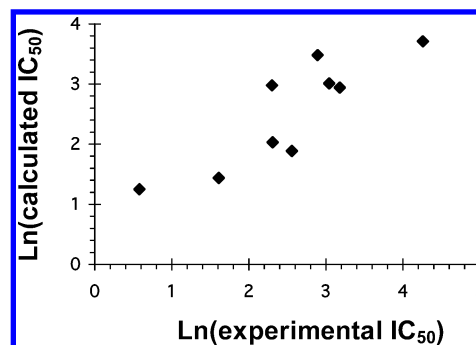


Figure 4. Predictive fragment QSAR for isosteric replacements of hydrogen-bond acceptor region (components 1 and 2) in Figure 2 performed on 3-Cl-AHPC carboxylate and other polar termini shown in Table 3 and based on IC₅₀ values for inhibition of MDA-MB-231 breast cancer proliferation after 96 h of treatment. The natural log of the antiproliferative activity in terms of IC₅₀ values would be expressed as $4.14 - 0.30L + 14.9\text{MINIM_PS} + 0.10\text{POLAR_V}$, where L is the longest length of the polar fragment; MINIM_PS is the minimum in the electrostatic potential on the van der Waals surface; and POLAR_V is volume of polar group, $R^2 \pm \text{SE} = 0.75 \pm 0.6$.

pothesized that the effects of **1** as well as those of 5-Cl-AHPN (**2**) and 3-Cl-AHPC (**5**) could be due to inhibition of an enzyme. Pfahl and Piedrafita subsequently reported that the IC₅₀ value obtained for **1** in inhibiting the dual-specificity mitogen-activated protein kinase phosphatase (MKP)-1 in vitro was in the 6-μM range.⁶¹ Because of their report, we investigated the inhibitory activity of several analogues of **5** on the protein-tyrosine phosphatases (PTPs) SHP-2 and CD45, both of which are implicated in the development of some forms of leukemia. Somatic gain-of-function mutations were found to occur in the PTPN11 gene for the cytoplasmic Src-homology 2 domain-containing PTP (SHP-2) in juvenile myelomonocytic leukemia and lead to hyperactivation of oncogenic Ras.^{62,63} Phosphorylated (activated) SHP-2 was reported to be overexpressed in 23 of 25 peripheral blood or bone marrow samples from adult chronic myeloid myelocytic leukemia patients but was only poorly or not expressed in samples from normal adults.⁶⁴ In addition, SHP-2 was observed to coimmunoprecipitate with phosphatidylinositol-3 kinase (PI3-K) in BCR-ABL tyrosine kinase-transformed cells.⁶⁵ In earlier work, we had observed that **5** was able to inhibit the PI3-K/Akt pathway in cancer cells.⁶⁶ The KG-1 leukemia cell line is reported to express SHP-2.⁶⁴ These observations suggested that inhibition of SHP-2 activity could affect KG-1 cell function and prompted us to investigate the effects of **5**, **31**, and **43** on KG-1 cells. Both **31** and **43** were found to inhibit SHP-2 PTP activity (Figure 5A) with IC₅₀ values of 1.3 μM and 2.2 μM, respectively, and, therefore, could serve as leads for the development of more potent and selective inhibitors of this enzyme. The IC₅₀ value for **5** was found to be 2.1 μM. This small sample did not permit us to correlate KG-1 growth inhibition with inhibition of enzyme activity.

CD45 PTP is found on the surface of cells of lymphohematopoietic lineage, including leukemia cells,⁶⁷ and the expression of its isoforms is altered in acute myeloid leukemia.^{67,68} We observed that AHPC (**4**), **31**, and **43** at 10 μM inhibited CD45 activity by 84%, 46%, and 53%, respectively, when dimethylformamide was used as the vehicle. 3-Cl-AHPC (**5**) and **60** were not evaluated. However, because **45**, **48**, and **57** had similar CD45 inhibitory activities (68%, 37%, and 54%, respectively) under these same conditions but at 5 μM were not able to inhibit KG-1 cell proliferation, the probability that **4**, **31**, and **43** inhibit KG-1 proliferation by inhibiting CD45 activity appears to be very low. As shown in the dose-response curve of Figure 5B,

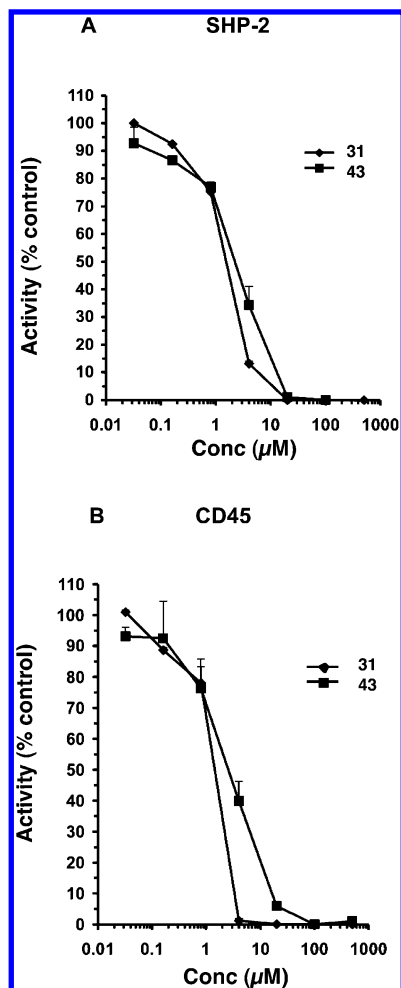


Figure 5. 3-Cl-AHPC analogues **31** and **43** inhibit the activity of SHP-2 and CD45 protein tyrosine phosphatases in cleaving 6,8-difluoro-4-methylumbelliferyl phosphate (100 μM) as measured by fluorescence spectrometry of the cleavage product as described in the Experimental Section. SHP-2 and CD45 concentrations were 5 nM and 1 nM, respectively. Tetrazole **31**, solid diamond; thiazolidinedione **43**, solid square. Results shown are the average of duplicates ± SE.

IC₅₀ values for CD45 PTP activity inhibition by **31** and **43** were 1.2 μM and 2.3 μM, respectively, when dimethyl sulfoxide was used as the vehicle.

Cancer cells stimulate angiogenesis to promote tumor growth and metastasis. In the presence of growth factors released by tumors and their related stroma, human microvascular endothelial (HMVE) cells from the surrounding vasculature are induced to proliferate, migrate into the tumor, and assemble into microtubular vessels. Because cancer cells underwent both cell-cycle arrest and apoptosis in response to 3-Cl-AHPC (**5**) and 5-Cl-AHPN (**2**), we wondered whether proliferating primary HMVE cells would behave similarly in culture. As shown in Figure 6, **5** effectively reduced HMVE cell growth (IC₅₀ = 0.3 μM). Thiazolidinedione **43** had low inhibitory activity (30% inhibition at 1.0 μM), whereas **24**, **31**, and **39** had no significant effect on HMVE cell growth compared to that of the vehicle-treated control.

We next examined whether 3-Cl-AHPC (**5**) would induce the apoptosis of proliferating HMVE cells in culture. Although no obvious cell detachment or rounding was observed after a 20-h incubation with **5**, oligonucleosome levels were significantly enhanced after treatment with 0.25 or 0.50 μM **5** in a concentration-dependent manner, as shown in Figure 7. These results demonstrate that **5** is able to induce HMVE cell

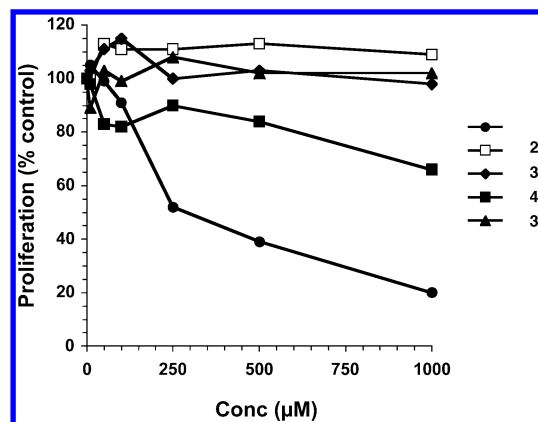


Figure 6. 3-Cl-AHPC (**5**) inhibits HMVE cell proliferation, whereas **43** is a poor inhibitor and **24**, **31**, and **39** do not inhibit. Cells were treated for 72 h at the indicated compound concentrations or with vehicle alone (Me₂SO), detached by trypsinization and counted as described in the Experimental Section. A representative experiment is shown with proliferation expressed as the percent of vehicle alone-treated control.

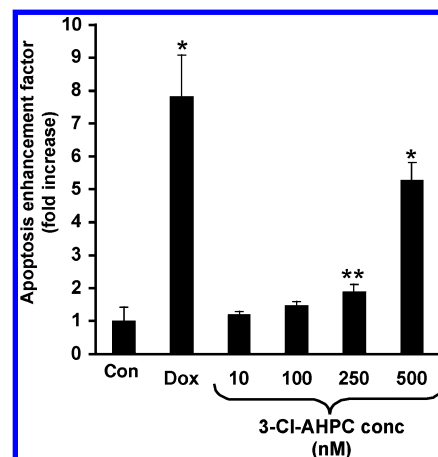


Figure 7. 3-Cl-AHPC (**5**) induces apoptosis of HMVE cells. Cells were incubated for 20 h in the presence of Me₂SO (negative control), positive control doxorubicin (1.0 μM), or **5** (10 nM to 500 nM) and assayed for apoptosis using a cell death detection ELISA as described in the Experimental Section. Values represent the enrichment of mono- and oligonucleosome levels in treated sample relative to Me₂SO control, and each bar represents the mean ± SD. Statistically significant differences (Student's *t*-test) compared with Me₂SO control are indicated (*, *p* < 0.05; **, *p* < 0.001).

apoptosis. Apoptosis induced by 0.5 μM **5** was 64% of that induced by 1.0 μM adriamycin. These results suggest that **5** has potential in vivo antiangiogenic activity.

3-Cl-AHPC (**5**) was further examined for its effects on HMVE cell migration and tubule formation. As shown in Figure 8, 0.05 nM to 0.50 μM **5** had no statistically significant effect on cell migration through Matrigel when cells were treated for 5-h compared to cells treated with only vehicle. Moreover, 18-h treatment with 0.25 μM or 1.0 μM **5** had no statistically significant effects on either the level of tube formation or tube length in Matrigel by cells obtained from 80% confluent cultures (Figure 9). In contrast, trans-RA (**7**) and other classical retinoids are reported to inhibit angiogenesis in chick chorioallantoic membrane.⁶⁹ To establish that these compounds were not exerting their effects through any retinoid-mediated pathway, the antiproliferative activity of AHPN (**1**) was compared to those of trans-RA (**7**), RARγ-selective transcriptional agonist SR11254 (**13**),^{70,71} and RARγ-selective antagonist SR11253 (**14**)^{70,71} in HMVE cells. The results shown in Table 2 demonstrate that **1** was the most potent of the four compounds, although it was

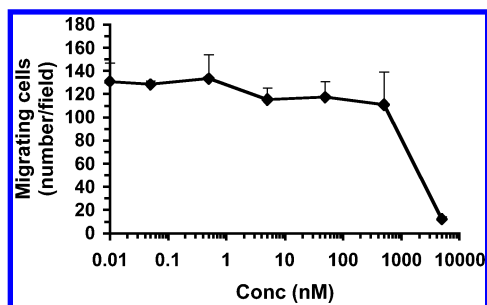


Figure 8. 3-Cl-AHPC (**5**) does not inhibit HMVE cell migration. Migration through Matrigel was measured after 5-h incubation with the indicated concentrations of **5** or with vehicle alone as described in the Experimental Section. Results shown represent the mean number of cells \pm SD of three fields in three replicates examined microscopically.

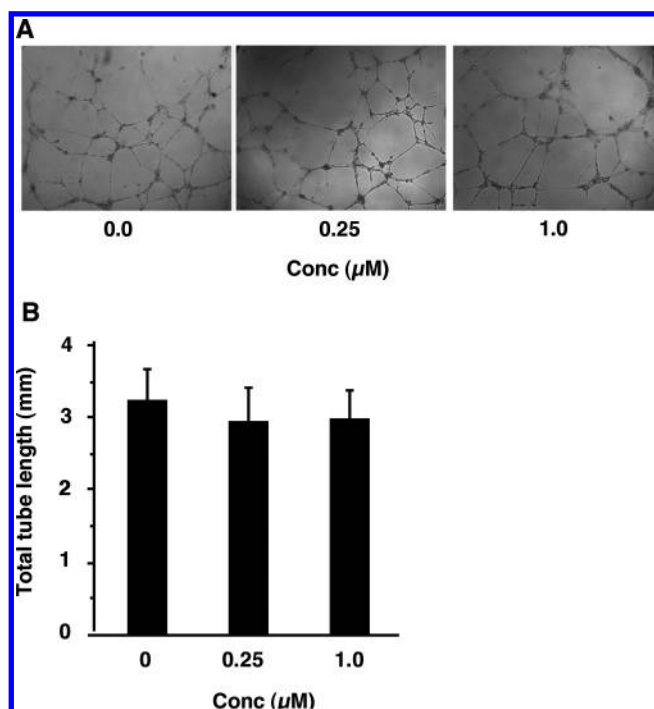


Figure 9. 3-Cl-AHPC (**5**) does not inhibit HMVE cell tubule formation or affect tube length. Cells in medium were layered onto Matrigel containing 0.25 μ M or 1.0 μ M **5**, which was added as a Me₂SO solution, or Me₂SO alone. Tube formation was examined microscopically as described in the Experimental Section. (A) Results shown are representative of one field of four in triplicate experiments. (B) Total tube length was determined in four random fields for each triplicate experiment. Bars represent the means \pm SD.

less efficient as a transactivator of the RARs than **7**.¹ 5-Cl-AHPN (**2**), AHPN (**4**), and **5** were also able to inhibit the proliferation of HMVE cells. In contrast, the 3-naphthalenecarboxylic acid and 2-naphthol analogues (**11** and **12**) of **1** were poor inhibitors of HMVE cell proliferation, just as they were of cancer cell growth.

Recently, we discovered that 3-Cl-AHPC (**5**) binds to the small heterodimer partner (SHP) nuclear orphan receptor.¹⁴ Interestingly, prior to its inducing the intrinsic apoptosis cascade in KG-1 AML and MDA-MB-231 breast cancer cells, **5** was found to interact with SHP in the nuclear Sin3A repressor complex. A recombinantly expressed glutathione *S*-transferase–SHP chimeric protein (GST–SHP) also bound **5**, as evidenced by its ability to displace tritiated AHPN⁴² from GST–SHP bound to glutathione-linked Sepharose beads, as did AHPN (**1**) and the 3-chlorophenyltetrazole and 3-chlorobenzylidenethiazolidinedione analogues (**39** and **43**, respectively). The relative

competitive displacement efficiencies of the tritiated label were as follows: nonlabeled **1**, 53%; **5**, 87%; 3-A-AHPC (**6**), 72%; tetrazole **39**, 69%; thiazolidinedione **43**, 37%; hydroxamic acid **48**, 7%; and boronic acid **57**, 0% at 50 μ M.

Conclusion

Thus, 3-Cl-AHPC (**5**) appears to negatively impact cancer cell growth through two signaling pathways, namely inhibiting cell proliferation and inducing apoptosis. Our results suggest that **5** also has antiangiogenic activity by modulating the same pathways in tumor microvasculature. The present fragment-based QSAR study on the hydrogen bond-accepting elements 1 and 2 of the pharmacophoric model shown in Figure 2A indicates that the dimensions of the elements and their minima in computed electrostatic potential on the van der Waals surface of the fragments have a major role in determining growth inhibitory activity. Defining the apoptotic activity properties of these elements was not possible because the present isosteric modifications of the carboxylate group abrogated apoptosis induction. These results suggest that if interaction with SHP regulates apoptotic activity, the region of SHP to which the carboxylate group binds is sterically constrained. Of the three hydrogen-acceptor analogues (**5**, **31**, and **43**) evaluated as inhibitors of phosphatases, only **5** was a potent inhibitor of both apoptosis and cell growth. Analogues **31** and **43** were only modest inhibitors of cell proliferation. Thus, while the present results suggest that inhibition of phosphatase activity may have a role in inhibition of cell proliferation, further studies will be necessary before robust conclusions can be drawn.

As observed with 3-A-AHPC (**6**), tetrazole **39** was able to compete with radiolabeled AHPN for binding to recombinantly expressed small heterodimer partner protein¹⁴ but was unable to induce KG-1 AML cell apoptosis. Earlier, we found that **6** was able to attenuate apoptosis induced by 3-Cl-AHPC (**5**).⁶ These results suggest that both **6** and **39** can function as antagonists of the apoptotic activity of **5**. Thus, with identified potent agonists (**1** and **5**) and antagonists (**6** and **39**) of SHP–Sin3A-mediated apoptotic activity, we plan on pursuing our studies on how these compounds regulate transcriptional signaling through SHP. Because both **31** and **43** exhibited similar modest antiproliferative activities but had very low apoptosis-inducing activity, they may have application as probes of the pathway by which **5** induces cell-cycle arrest independent of apoptosis.

Experimental Section

Chemistry. Chemicals and solvents from commercial sources were used without further purification unless specified. Abbreviations for solvents and reagents are as follows: DIBAL, diisobutylaluminum hydride; DIC, diisopropylcarbodiimide; DMAP, 4-(*N,N*-dimethylamino)pyridine; DMF, dimethylformamide; DME, ethylene glycol dimethyl ether; TBAF, tetra(*n*-butyl)ammonium fluoride; THF, tetrahydrofuran; Tf₂O, trifluoromethanesulfonic anhydride. Reactions were carried out under argon and monitored by thin-layer chromatography on silica gel (mesh size 60, F₂₅₄) with visualization under UV light. Organic extracts were dried over Na₂SO₄ unless otherwise specified and concentrated at reduced pressure. Standard and flash column chromatography employed silica gel (Merck 60, 230–400 mesh). Experimental procedures were not optimized. Melting points for samples were determined in capillaries using a Mel-Temp II apparatus and are uncorrected. Infrared spectra were obtained using an FT-IR Mason satellite spectrophotometer on powdered samples. ¹H NMR spectra were recorded on a 300-MHz Varian Unity Inova spectrometer, and shift values are expressed in ppm (δ) relative to CHCl₃ as an internal standard. Unless mentioned otherwise, compounds were dissolved in ²HClCl₃. MALDI-FAB mass spectra were run on an Applied Biosystems

Voyager De-Pro MALDI-TOF instrument at the Burnham Institute. High-resolution mass spectra were recorded on an Agilent ESI-TOF mass spectrometer at The Scripps Research Institute (La Jolla, CA). Electrospray mass spectrometry was performed on an ABI EPI-3000 instrument.

3-(1-Adamantyl)-4-benzyloxyphenylboronic Acid (16).³⁵ Our reported procedure⁸ was adapted. To a solution of 3-(1-adamantyl)-4-benzyloxyphenyl bromide⁸ (2.00 g, 5.04 mmol) in THF (7 mL) at -78°C (dry ice/acetone bath) under argon was added in one portion 1.6 M *n*-BuLi (7.56 mmol) in hexane (4.7 mL). The mixture was stirred at -78°C for 15 min, (*i*-PrO)₃B (3.5 mL, 15.1 mmol) was added, and the resulting solution was stirred at -78°C for 20 min and then at room temperature overnight. The mixture was quenched with 0.1 N HCl (30 mL) and extracted with EtOAc (3 \times 190 mL). The extracts were washed (brine) and dried. The residue after concentration was purified on silica gel (40% EtOAc/hexane) to give 1.63 g (89%) of **16** as a white solid, mp $151\text{--}153^{\circ}\text{C}$. ¹H NMR δ 1.78 (bs, 6H, AdCH₂), 2.09 (bs, 3H, AdCH), 2.27 (bs, 6H, AdCH₂), 5.23 (s, 2H, ArCH₂), 7.07 (d, $J = 8.1$ Hz, 1H, 5-ArH), 7.33–7.55 (m, 5H, ArH), 8.04 (dd, $J = 8.1, 1.5$ Hz, 1H, 6-ArH), 8.2 ppm (d, $J = 1.2$ Hz, 1H, 2-ArH).

4-Benzyloxy-3-chlorobenzaldehyde (18).⁷² To a suspension of **17** (4.68 g, 30 mmol) and K₂CO₃ (6.90 g, 50 mmol) in THF (50 mL) and DMF (10 mL) under argon was added benzyl bromide (6.84 g, 40 mmol). The mixture was heated at reflux for overnight, concentrated, diluted with CH₂Cl₂ (100 mL), washed (water, 1 N HCl and brine), and dried. Concentration and chromatography (15% EtOAc/hexane) afforded 6.22 g (84%) of **18** as a white solid; mp $92\text{--}94^{\circ}\text{C}$. IR (CHCl₃) 2966, 1682 cm⁻¹; ¹H NMR δ 5.23 (s, 2H, ArCH₂), 7.08 (d, $J = 8.4$ Hz, 1H, 5-ArH), 7.35–7.46 (m, 5H, ArH), 7.74 (d, $J = 6.6$ Hz, 1H, 6-ArH), 7.94 (d, $J = 1.5$ Hz, 1H, 2-ArH), 9.85 ppm (s, 1H, CHO).

(E)-4-Benzyloxy-3-chlorocinnamionitrile (19). To diethyl (cyanomethyl)phosphonate (885 mg, 5.0 mmol) in THF (5 mL) stirred with cooling in a dry ice/acetone bath was added under argon 10 mL of 0.5 M KN(SiMe₃)₂ (5.0 mmol) in toluene. Stirring was continued for 0.5 h before **18**⁷² (738 mg, 3.0 mmol) in THF (5.0 mL) was slowly added over a 0.5-h period. After being stirred for 1 h more, the mixture was allowed to warm to room temperature, stirred overnight, poured into 1 M NH₄Cl (10 mL) and water (20 mL), and extracted with hexane (100 mL). The extract was washed (water and brine) and dried. Concentration and chromatography on silica gel (EtOAc/hexane) afforded 710 mg (91%) of **19** as a white powder, *R*_f 0.47 (EtOAc/hexane); mp $110\text{--}114^{\circ}\text{C}$. IR (CHCl₃) 2966, 2215 cm⁻¹; ¹H NMR δ 5.21 (s, 2H, ArCH₂), 5.73 (d, $J = 15.9$ Hz, 1H, HC=CCN), 6.97 (d, $J = 8.4$ Hz, 1H, 5-ArH), 7.26 (d, $J = 16.5$ Hz, 1H, C=CHCN), 7.36–7.45 (m, 6H, ArH, 6-ArH), 7.51 ppm (d, $J = 2.1$ Hz, 1H, 2-ArH). The crude nitrile was converted directly to **20**.

General Procedure for Debenzylation of 19, 22, 26, 29, 32, 38, 42, 44, 47, 56, 59, and 61. To a stirred mixture of the benzyl ether (2.5 mmol) in CH₂Cl₂ (10 mL) at -78°C under argon was added slowly over a 10-min period 6.0 mL of 1.0 M BBr₃ (6.0 mmol) in CH₂Cl₂. The mixture was stirred for 2 h at -78°C . Water (10 mL) was added, and the mixture was stirred for 10 min and then extracted (EtOAc). The extract was washed (water and brine), dried, and concentrated. Flash chromatography of the residue on silica gel (10% EtOAc/hexane) yielded the phenol.

(E)-3-Chloro-4-hydroxycinnamionitrile (20). **19** (672 mg, 2.5 mmol) yielded 420 mg (94%) of **20** as a pale-yellow powder, *R*_f 0.12 (10% EtOAc/hexane); mp $165\text{--}169^{\circ}\text{C}$. IR (powder) 3416, 2966, 2213 cm⁻¹; ¹H NMR δ 6.32 (d, $J = 16.2$ Hz, 1H, HC=CHCN), 7.02 (dd, $J = 3.0, 8.7$ Hz, 1H, 5-ArH), 7.48 (d, $J = 10.2$ Hz, 1H, 6-ArH), 7.54 (d, $J = 16.2$ Hz, 1H, HC=CHCN), 7.75 (s, 1H, 2-ArH), 10.88 ppm (s, 1H, OH). The crude product was converted directly to the triflate **21**.

(E)-4-[3'-(1-Adamantyl)-4'-hydroxyphenyl]-3-chlorocinnamionitrile (23). **22** (420 mg, 87 mmol) yielded 310 mg (87%) of **23** as a pale-yellow solid, *R*_f 0.15 (5% EtOAc/hexane); mp $142\text{--}148^{\circ}\text{C}$, which was used to prepare **24**. IR (CHCl₃) 3394, 2906, 2226, 1284 cm⁻¹; ¹H NMR δ 1.80 (s, 6H, AdCH₂), 2.10 (s, 3H, AdCH), 2.16

(s, 6H, AdCH₂), 5.00 (s, 1H, OH), 5.90 (d, $J = 17.1$ Hz, 1H, HC=CHCN), 6.72 (d, $J = 7.8$ Hz, 1H, 5'-ArH), 7.17 (dd, $J = 2.1, 8.1$ Hz, 1H, 6'-ArH), 7.32 (d, $J = 9.3$ Hz, 1H, 6-ArH), 7.33 (d, $J = 18.0$ Hz, 1H, CH=CHCN), 7.38 (s, 1H, 2'-Ar), 7.39 (d, $J = 7.8$ Hz, 1H, 6-ArH), 7.55 ppm (d, $J = 1.8$ Hz, 1H, 3-ArH).

3-Chloro-4-hydroxybenzonitrile (27). **26** (850 mg, 3.5 mmol) yielded after chromatography (20% EtOAc/hexane) (470 mg, 88%) of phenol **27** as a pale-yellow solid, which was converted directly to triflate **28**.

4-[3'-(1-Adamantyl)-4'-hydroxyphenyl]-3-chlorobenzonitrile (30). **29** (300 mg, 0.66 mmol) yielded 0.45 g (87%) of **30** as a pale-yellow solid, *R*_f 0.37 (10% EtOAc/hexane); mp $220\text{--}222^{\circ}\text{C}$. IR (CHCl₃) 3410, 2966, 2237, 1278 cm⁻¹; ¹H NMR δ 1.80 (s, 6H, AdCH₂), 2.10 (s, 3H, AdCH), 2.15 (s, 6H, AdCH₂), 5.02 (s, 1H, OH), 6.74 (d, $J = 8.4$ Hz, 1H, 5'-ArH), 7.17 (dd, $J = 8.1, 2.1$ Hz, 1H, 6'-ArH), 7.30 (d, $J = 2.4$ Hz, 1H, 2'-ArH), 7.44 (d, $J = 7.8$ Hz, 1H, 5-ArH), 7.57 (dd, $J = 7.8, 1.5$ Hz, 1H, 6-ArH), 7.75 ppm (d, $J = 1.5$ Hz, 1H, 2-ArH). FTMS (HRMS) calcd C₂₃H₂₃-ClNO [M + H]⁺ expected 364.1463, found 364.1461.

Ethyl (E)-3-Chloro-4-hydroxycinnamate (33).⁸ **32**⁷² yielded after chromatography (24% EtOAc/hexane) 0.855 g (92%) of **33** as a white solid, mp $106\text{--}108^{\circ}\text{C}$. ¹H NMR δ 1.34 (t, $J = 7.2$ Hz, 3H, CH₂CH₃), 4.26 (q, $J = 7.2$ Hz, 2H, CH₂CH₃), 5.84 (s, 1H, OH), 6.32 (d, $J = 16.2$ Hz, 1H, CH=CHCO), 7.04 (d, $J = 8.4$ Hz, 1H, 5-ArH), 7.37 (dd, $J = 8.4, 2.1$ Hz, 1H, 6-ArH), 7.52 (d, $J = 1.8$ Hz, 1H, 2-ArH), 7.58 ppm (d, $J = 16.2$ Hz, 1H, CH=CHCO). The product was used directly in the next step.

5-[3-(3'-(1-Adamantyl)-2-chloro-4'-hydroxy-4-biphenyl)-(2E)-2-propenylidene]-2,4-thiazolidinedione (39). **38** (35 mg, 0.06 mmol) yielded 25 mg (85%) of **39** as an orange powder, *R*_f 0.27 (30% EtOAc/hexane); mp $162\text{--}164^{\circ}\text{C}$ (dec). IR (CHCl₃) 3394, 2912, 1695, 1601, 1278 cm⁻¹; ¹H NMR (C₂H₅O₂H) δ 1.78 (s, 6H, AdCH₂), 2.07 (s, 3H, AdCH), 2.17 (s, 6H, AdCH₂), 6.80 (d, $J = 8.1$ Hz, 1H, 5'-ArH), 6.91 (dd, $J = 15.9, 11.4$ Hz, 1H, ArCH=CHCH=C), 7.12 (dd, $J = 7.8, 2.1$ Hz, 1H, 6'-ArH), 7.16 (d, $J = 15$ Hz, 1H, ArCH=CHCH=C), 7.26 (d, $J = 2.1$ Hz, 1H, 2'-ArH), 7.38 (d, $J = 8.1$ Hz, 1H, 5-ArH), 7.52 (d, $J = 11.4$ Hz, 1H, ArCH=CHCH=C), 7.58 (dd, $J = 8.1, 1.8$ Hz, 1H, 6-ArH), 7.70 ppm (d, $J = 1.8$ Hz, 1H, 2-ArH). HRMS calcd C₂₈H₂₆ClNO₃S [M - H]⁻ 490.1249, found 490.1245.

5-{4-[3'-(1-Adamantyl)-4'-hydroxyphenyl]-3-chlorobenzylidene}-2,4-thiazolidinedione (43). **42** (12 mg, 0.02 mmol) yielded after chromatography (20% EtOAc/hexane) 8.3 mg (91%) of **43** as a yellow powder, *R*_f 0.36 (20% EtOAc/hexane); mp $280\text{--}284^{\circ}\text{C}$. IR (CHCl₃) 3372, 2902, 1655, 1577 cm⁻¹; ¹H NMR (C₂H₅O₂H) δ 1.85 (s, 6H, AdCH₂), 2.08 (s, 3H, AdCH), 2.22 (d, $J = 2.4$ Hz, 6H, AdCH₂), 6.82 (d, $J = 8.1$ Hz, 1H, 5'-ArH), 7.16 (dd, $J = 8.4, 1.8$ Hz, 1H, 6'-ArH), 7.28 (d, $J = 2.4$ Hz, 1H, 2'-ArH), 7.50 (d, $J = 8.1$ Hz, 1H, 5-ArH), 7.55 (d, $J = 8.1$ Hz, 1H, 6-ArH), 7.68 (s, 1H, 2-ArH), 7.80 ppm (s, 1H, ArCH=C). HRMS calcd C₂₆H₂₄-ClNO₃S [M - H]⁻ 464.1093, found 464.1107.

2-[3-(1-Adamantyl)-2-chloro-4'-hydroxy-4-biphenyl]methylene]-propanedinitrile (45). **44** (74 mg, 0.15 mmol) yielded after chromatography (20% EtOAc/hexane) 42.5 mg (70%) of **45** as a yellow solid, mp $225\text{--}226^{\circ}\text{C}$. IR 3450, 2901, 2848, 2230, 1276 cm⁻¹; ¹H NMR δ 1.80 (bs, 6H, AdCH₂), 2.11 (bs, 3H, AdCH), 2.15 (bs, 6H, AdCH₂), 5.08 (s, 1H, OH), 6.76 (d, $J = 8.4$ Hz, 1H, 5'-ArH), 7.24 (dd, $J = 7.8, 2.4$ Hz, 1H, 6'-ArH), 7.36 (d, $J = 1.8$ Hz, 1H, 5-ArH), 7.53 (d, $J = 7.8$ Hz, 1H, 2'-ArH), 7.74 (s, 1H, CH=C(CN)₂), 7.90–7.94 ppm (m, 2H, 3-ArH, 6-ArH). HRMS calcd C₂₆H₂₃ClN₂O [M - H]⁻ 413.1426, found 413.1418.

N-(Hydroxy) (E)-4-[3'-(1-Adamantyl)-4'-hydroxyphenyl]-3-chlorocinnamamide (48). **47** (70 mg, 0.117 mmol) yielded after chromatography (HOAc/EtOAc/hexane, 0.3:10:10) 22 mg (45%) of **48** as a pale-tan solid, mp 208°C (dec). IR 3334, 2899, 1652, 1382 cm⁻¹; ¹H NMR [(C₂H₅)₂SO] δ 1.75 (bs, 6H, AdCH₂), 2.04 (bs, 3H, AdCH), 2.16 (bs, 6H, AdCH₂), 6.65 (d, $J = 15.9$ Hz, 1H, CH=CHCO), 6.88 (d, $J = 8.1$ Hz, 1H, 5'-ArH), 7.12 (dd, $J = 8.1, 1.8$ Hz, 1H, 6'-ArH), 7.16 (d, $J = 1.8$ Hz, 1H, 2'-ArH), 7.41 (s, 1H, 3-ArH), 7.50 (d, $J = 15.9$ Hz, 1H, CH=CHCO), 7.55 (d, $J = 8.4$ Hz, 1H, 5-ArH), 7.71 (d, $J = 8.4$ Hz, 1H, 6-ArH), 9.63 (bs,

1H, OH), 9.69 (bs, 1H, N HOH), 10.81 ppm (bs, 1H, NHO H). HRMS calcd $C_{25}H_{26}ClNO_3$ [M + H]⁺ 424.1674, found 424.1669. **(E)-2-[3'-(1-Adamantyl)-2-chloro-4'-hydroxy-4-biphenyl]-ethenylboronic Acid (57)**. **56** (56 mg, 0.097 mmol) yielded after chromatography (50% EtOAc/hexane) 31 mg (67%) of **57** as a pale-tan solid, mp 186–189 °C. IR 3350, 2901, 1621, 1217 cm⁻¹; ¹H NMR δ 1.81 (bs, 6H, AdCH₂), 2.11 (bs, 3H, AdCH), 2.18 (m, 6H, AdCH₂), 4.92 (s, 1H, OH), 6.38 (d, *J* = 18 Hz, 1H, CH=CHB), 6.74 (d, *J* = 8.1 Hz, 1H, 5'-ArH), 7.22 (dd, *J* = 8.4, 2.1 Hz, 1H, 6'-ArH), 7.36 (d, *J* = 2.1 Hz, 1H, 2'-ArH), 7.39 (d, *J* = 8.1 Hz, 1H, 6-ArH), 7.55 (dd, *J* = 8.1, 1.5 Hz, 1H, 5-ArH), 7.73 (d, *J* = 1.5 Hz, 1H, 3-ArH), 7.76 ppm (d, *J* = 18 Hz, 1H, CH=CHB). HRMS calcd $C_{24}H_{26}BClO_3$ [M + H]⁺ 409.1736, found 409.1730. **(3E)-4-[3'-(1-Adamantyl)-2-chloro-4'-hydroxy-4-biphenyl]-2-oxobut-3-enal (60)**. **59** (35 mg, 0.068 mmol) yielded after chromatography (25% to 33% EtOAc/hexane) 22 mg (77%) of **60** as a yellow wax, mp 121–123 °C. IR 3383, 2902, 1695, 1678, 1603, 1251 cm⁻¹; ¹H NMR δ 1.80 (bs, 6H, AdCH₂), 2.11 (bs, 3H, AdCH), 2.16 (bs, 6H, AdCH₂), 5.10 (s, 1H, OH), 6.74 (d, *J* = 8.1 Hz, 1H, 5'-ArH), 6.97 (d, *J* = 16.2 Hz, 1H, CH=CHCO), 7.20 (dd, *J* = 8.4, 2.1 Hz, 1H, 6'-ArH), 7.34 (d, *J* = 2.1 Hz, 1H, 2'-ArH), 7.41 (d, *J* = 8.1 Hz, 1H, 6-ArH), 7.52 (dd, *J* = 8.1, 2.1 Hz, 1H, 5-ArH), 7.71 (d, *J* = 1.5 Hz, 1H, 3-ArH), 7.80 (d, *J* = 16.2 Hz, 1H, CH=CHCO), 9.47 ppm (s, 1H, CHO). HRMS calcd $C_{26}H_{25}ClO_3$ [M + H]⁺ 421.1565, found 421.1573.

Diethyl (E)-2-[3'-(1-Adamantyl)-2-chloro-4'-hydroxy-4-biphenyl]ethenylphosphonate (62). **61** (0.14 mmol, 82 mg) yielded after chromatography (50% to 67% EtOAc/hexane) 61 mg (87%) of **62** as an off-white solid, mp 110–112 °C. IR 3414, 2932, 1028, 989 cm⁻¹; ¹H NMR δ 1.38 (t, *J* = 6.9 Hz, 6H, OCH₂CH₃), 1.79 (bs, 6H, AdCH₂), 2.09 (bs, 3H, AdCH), 2.17 (bs, 6H, AdCH₂), 4.18 (m, 4H, OCH₂CH₃), 6.29 (t, *J* = 17.4 Hz, 1H, CH=CHP), 6.82 (d, *J* = 8.4 Hz, 1H, 5'-ArH), 7.17 (dd, *J* = 8.4, 2.1 Hz, 1H, 6'-ArH), 7.31 (d, *J* = 2.1 Hz, 1H, 2'-ArH), 7.33–7.41 (m, 3H, 5-ArH, 6-ArH, OH), 7.48 (dd, *J* = 17.4, 22.5 Hz, 1H, CH=CHP), 7.59 ppm (s, 1H, 3-ArH). HRMS calcd $C_{28}H_{34}ClO_4P$ [M + H]⁺ 501.1956, found 501.1958.

General Procedure for Converting Phenols 20, 27, 33, 17, and 49 to Their Triflates. To a stirred solution of the phenol (2.0 mmol) in pyridine (5 mL) at 0 °C (ice-bath) under argon was slowly added Tf₂O (846 mg, 3.0 mmol) over a 0.5-h period. The reaction mixture was stirred at room temperature overnight and then extracted (EtOAc). The extract was washed (10% HCl, 5% NaHCO₃, brine and water), dried, and concentrated to afford an oil, which was purified by chromatography (5% EtOAc/hexane) to give the triflate. **(E)-3-(3-Chloro-4-trifluoromethanesulfonyloxy)cinnamionitrile (21)**. **20** (358 mg, 2.0 mmol) gave 565 mg (91%) of **21** as a white powder, *R*_f 0.68 (10% EtOAc/hexane); mp 93–99 °C. IR (CHCl₃) 2966, 2226 cm⁻¹; ¹H NMR δ 5.93 (d, *J* = 16.5 Hz, 1H, HC=CHCN), 7.34 (d, *J* = 16.8 Hz, 1H, HC=CHCN), 7.42 (s, 2H, 5,6-ArH), 7.62 ppm (s, 1H, 2-ArH). The crude product was used to prepare **22**.

3-Chloro-4-(trifluoromethanesulfonyloxy)benzonitrile (28). Crude **27** (306 mg, 2.0 mmol) gave 530 mg (93%) of **28** as a white powder, *R*_f 0.80 (20% EtOAc/hexane); mp 55–56 °C, which was used directly for coupling to produce **29**. IR (CHCl₃) 2961, 2243 cm⁻¹; ¹H NMR δ 7.50 (d, *J* = 8.7 Hz, 1H, 5-ArH), 7.69 (dd, *J* = 8.1, 1.8 Hz, 1H, 6-ArH), 7.86 ppm (s, 1H, 2-ArH).

Ethyl (E)-3-Chloro-4-(trifluoromethanesulfonyloxy)cinnamate (34). **33** (800 mg, 3.54 mmol) gave 1.13 g (93%) of **34** as a white solid, *R*_f 0.62 (10% EtOAc/hexane); mp 78–80 °C. IR (CHCl₃) 2961, 1706, 1651, 1432 cm⁻¹; ¹H NMR δ 1.35 (t, *J* = 6.9 Hz, 3H, CH₃), 4.29 (q, *J* = 7.2 Hz, 2H, OCH₂), 6.44 (d, *J* = 15.9 Hz, 1H, HC=CHCO), 7.39 (d, *J* = 8.4 Hz, 1H, 5-ArH), 7.48 (dd, *J* = 8.4, 1.8 Hz, 1H, 6-ArH), 7.60 (d, *J* = 16.2 Hz, 1H, CH=CHCO), 7.68 ppm (s, 1H, 2-ArH). HRMS calcd $C_{12}H_{10}ClF_3O_5S$ [M + H]⁺ 358.9962, found 358.9951.

3-Chloro-4-(trifluoromethanesulfonyloxy)benzaldehyde (40). **17** (1.56 g, 10.0 mmol) gave 2.30 g (79%) of **40** as a pale-yellow oil, *R*_f 0.65 (20% EtOAc/hexane). IR (CHCl₃) 2961, 1717, 1223 cm⁻¹; ¹H NMR δ 7.61 (d, *J* = 8.4 Hz, 1H, 5-ArH), 7.94 (dd, *J* = 8.6, 1.8

Hz, 1H, 6-ArH), 8.11 (d, *J* = 1.8 Hz, 1H, 2-ArH), 10.07 ppm (s, 1H, CHO). FTMS (HRMS) calcd $C_8H_5ClF_3O_4S$ [M + H]⁺ expected 288.9544, found 288.9542.

2-Chloro-4-nitrophenyl Trifluoromethanesulfonate (50). **49** (1.58 g, 9.12 mmol) gave after chromatography (12.5% EtOAc/hexane) 2.73 g (97%) of **50** as a yellow oil, which was used to prepare **51**. ¹H NMR δ 7.59 (d, *J* = 9 Hz, 1H, 6-ArH), 8.26 (dd, *J* = 9, 2.7 Hz, 1H, 5-ArH), 8.45 ppm (d, *J* = 2.7 Hz, 1H, 3-ArH).

General Procedure for the Coupling between Aryl Boronic Acid 16 and Aryl Triflates 21, 28, 34, 40, and 50. To a stirred suspension of the aryl triflate (1.6 mmol), **16** (651 mg, 1.8 mmol), Pd(PPh₃)₄ (115 mg, 0.1 mmol), and LiCl (242 mg, 2.8 mmol) in DME (8 mL) was added under argon 1.3 mL of 2.0 M aq Na₂CO₃ (2.6 mmol). The mixture was heated at reflux for 24 h, cooled, and extracted (EtOAc). The extract was washed (water and brine), dried, and concentrated. Flash chromatography on silica gel (5% EtOAc/hexane) yielded the diaryl-coupling product.

(E)-3-[3'-(1-Adamantyl)-4'-benzyloxyphenyl]-3-chlorocinnamionitrile (22). **21** (498 mg, 1.6 mmol) yielded 510 mg (64%) of **22** as a white solid, *R*_f 0.55 (5% EtOAc/hexane); mp 72–74 °C. IR (CHCl₃) 2906, 2221 cm⁻¹; ¹H NMR δ 1.75 (s, 6H, AdCH₂), 2.06 (s, 3H, AdCH), 2.20 (s, 6H, AdCH₂), 5.18 (s, 2H, ArCH₂), 5.91 (d, *J* = 16.8 Hz, 1H, CH=CHCN), 7.02 (d, *J* = 8.7 Hz, 1H, 5'-ArH), 7.28 (dd, *J* = 8.4, 2.1 Hz, 1H, 6'-ArH), 7.45–7.35 (m, 7H, ArH, 5-ArH, 2'-ArH), 7.48 (d, *J* = 16.8 Hz, 1H, CH=CHCN), 7.53 (d, *J* = 8.4 Hz, 1H, 6-ArH), 7.56 ppm (d, *J* = 1.5 Hz, 1H, 3-ArH). The crude product was used to prepare **23**.

4-[3'-(1-Adamantyl)-4'-benzyloxyphenyl]-3-chlorobenzonitrile (29). **28** (428 mg, 1.5 mmol) yielded 390 mg (57%) of **29** as a white solid, *R*_f 0.55 (5% EtOAc/hexane); mp 60–62 °C, which was used to prepare **30**. IR (CHCl₃) 2906, 2232 cm⁻¹; ¹H NMR δ 1.74 (s, 6H, AdCH₂), 2 (s, 3H, AdCH), 2.18 (s, 6H, AdCH₂), 5.18 (s, 2H, ArCH₂), 7.02 (d, *J* = 8.4 Hz, 1H, 5'-ArH), 7.27 (dd, *J* = 8.4, 2.1 Hz, 1H, 6'-ArH), 7.35–7.47 (m, 6H, 2'-ArH, ArH), 7.51 (d, *J* = 7.8 Hz, 1H, 5-ArH), 7.58 (dd, *J* = 8.1, 1.5 Hz, 1H, 6-ArH), 7.76 ppm (d, *J* = 1.5 Hz, 1H, 2-ArH).

Ethyl (E)-4-[3'-(1-Adamantyl)-4'-benzyloxyphenyl]-3-chlorocinnamate (35). **34** (500 mg, 1.40 mmol) yielded 1.33 g (91%) of **35** as a white solid, which was reduced to **36**. *R*_f 0.51 (10% EtOAc/hexane); mp 72–74 °C. IR (CHCl₃) 2906, 1713, 1640 cm⁻¹; ¹H NMR δ 1.35 (t, *J* = 7.2 Hz, 3H, CH₃), 1.72 (s, 6H, AdCH₂), 2.04 (s, 3H, AdCH), 2.17 (s, 6H, AdCH₂), 4.27 (q, *J* = 6.9 Hz, 2H, OCH₂), 5.17 (s, 2H, ArCH₂), 6.46 (d, *J* = 15.2 Hz, 1H, HC=CHCO), 7.00 (d, *J* = 8.1 Hz, 1H, 5'-ArH), 7.29 (d, *J* = 8.1 Hz, 1H, 6'-ArH), 7.35–7.42 (m, 5H, ArH), 7.43 (d, *J* = 6.9 Hz, 1H, 5-ArH), 7.50 (s, 1H, 2'-ArH), 7.52 (d, *J* = 7.2 Hz, 1H, 6-ArH), 7.62 (s, 1H, 2-ArH), 7.64 ppm (d, *J* = 15.3 Hz, 1H, CH=CHCO).

4-[3'-(1-Adamantyl)-4'-benzyloxyphenyl]-3-chlorobenzaldehyde (41). **40** (289 mg, 1.00 mmol) yielded after chromatography (10% EtOAc/hexane) 215 mg (78%) of **41** as a white solid, mp 115–116 °C. IR 2902, 1699, 1596, 1262 cm⁻¹; ¹H NMR δ 1.75 (bs, 6H, AdCH₂), 2.06 (bs, 3H, AdCH), 2.19 (bs, 6H, AdCH₂), 5.19 (s, 2H, ArCH₂), 7.04 (d, *J* = 8.4 Hz, 1H, 5'-ArH), 7.31–7.56 (m, 8H, 6-ArH, 2'-ArH, 6'-ArH, ArH), 7.81 (dd, *J* = 7.8, 1.5 Hz, 1H, 5-ArH), 7.99 (d, *J* = 1.5 Hz, 1H, 2-ArH), 10.01 ppm (s, 1H, CHO). HRMS calcd $C_{30}H_{29}ClO_2$ [M + Na]⁺ 479.1748, found 479.1763.

3'-(1-Adamantyl)-4'-benzyloxy-2-chloro-4-nitrobiphenyl (51). **50** (721 mg, 2.36 mmol) yielded after chromatography (7% EtOAc/hexane) 908 mg (81%) of **51** as a yellow solid, mp 52–54 °C, which was reduced to **52**. ¹H NMR δ 1.77 (bs, 6H, AdCH₂), 2.09 (bs, 3H, AdCH), 2.21 (m, 6H, AdCH₂), 5.21 (s, 2H, ArCH₂), 7.06 (d, *J* = 8.7 Hz, 1H, 5'-ArH), 7.32 (dd, *J* = 8.7, 2.1 Hz, 1H, 6'-ArH), 7.35–7.56 (m, 7H, 2'-ArH, 6-ArH, ArH), 8.16 (dd, *J* = 8.7, 2.4 Hz, 1H, 5-ArH), 8.37 ppm (d, *J* = 2.4 Hz, 1H, 3-ArH).

(E)-5-[2-[3'-(1-Adamantyl)-2-chloro-4'-hydroxy-4-biphenyl]ethenyl]-1H-tetrazole (24). A reported procedure⁷³ was applied. To **23** (78 mg, 0.2 mmol) in toluene (2 mL) were added (*n*-Bu)₂SnO (5.0 mg, 0.02 mmol) and azidotrimethylsilane (58 mg, 1.0 mmol). The mixture was stirred at 90–95 °C for 48 h. Additional azidotrimethylsilane (34 mg, 0.3 mmol) was added, and stirring

was continued for 20 h. The mixture was concentrated, diluted with EtOAc (10 mL) and 10% HCl (3 mL), and stirred for 0.5 h. The organic layer was washed (water and brine) and dried. Concentration and crystallization (EtOAc/CH₂Cl₂/hexane) gave 55 mg (64%) of **24** as a white powder, *R_f* 0.28 (50% EtOAc/hexane); mp 260–262 °C. IR (CHCl₃) 3405, 2966, 2237 cm⁻¹; ¹H NMR (C²H₃O²H) δ 1.72 (s, 6H, AdCH₂), 2.01 (s, 3H, AdCH), 2.12 (s, 6H, AdCH₂), 7.09 (d, *J* = 16.5 Hz, 1H, CH=CH), 7.11 (d, *J* = 10.5 Hz, 1H, 5'-ArH), 7.22 (s, 1H, 2'-ArH), 7.28 (d, *J* = 8.1 Hz, 1H, 6'-ArH), 7.32 (d, *J* = 7.8 Hz, 1H, 5-ArH), 7.40 (d, *J* = 8.7 Hz, 1H, 6-ArH), 7.56 (s, 1H, 3-ArH), 7.61 ppm (d, *J* = 16.5 Hz, 1H, CH=CH). FTMS (HRMS) calcd C₂₅H₂₅ClN₄O (M + H)⁺ expected 433.1790, found 433.1801.

4-Benzoyloxy-3-chlorobenzonitrile (26). To a solution of **18** (1.23 g, 5 mmol) in MeOH (10 mL) and pyridine (2 mL) was added NH₂OH·HCl (695 mg, 10 mmol). The mixture was stirred at 50 °C under argon for 5 h and then poured into ice water to give a solid, which was collected by filtration, washed with water, and dried. Chromatography (9% EtOAc/hexane) gave 1.21 g (94%) of oxime **25** as a white solid, which was used for the elimination step.

To **25** (1.1 g, 4.2 mmol) in toluene (15 mL) and pyridine (2 mL) cooled in an ice bath was slowly added methanesulfonyl chloride (798 mg, 7 mmol) over a 10-min period. The mixture was stirred at reflux for 3 h, cooled to room temperature, and diluted with toluene (30 mL). The organic phase was washed (1 N HCl, 5% NaHCO₃, water, and brine) and dried. Concentration and chromatography (10% EtOAc/hexane) gave 910 mg (91%) of **26** as a white solid, *R_f* 0.60 (20% EtOAc/hexane); mp 120–122 °C. IR (CHCl₃) 2966, 2232 cm⁻¹; ¹H NMR δ 5.23 (s, 2H, ArCH₂), 7.0 (d, *J* = 8.7 Hz, 1H, 5-ArH), 7.35–7.45 (m, 5H, ArH), 7.50 (dd, *J* = 8.7, 2.1 Hz, 1H, 6-ArH), 7.68 ppm (d, *J* = 2.1 Hz, 1H, 2-ArH). The crude product was used directly in the next step.

5-[3'-(1-Adamantyl)-2-chloro-4'-hydroxy-4-biphenyl]-1H-tetrazole (31). A reported procedure was applied.⁷³ To **30** (73 mg, 0.2 mmol) in toluene (2 mL) was added (*n*-Bu)₂SnO (5.0 mg, 0.02 mmol) and azidotrimethylsilane (115 mg, 1.0 mmol). This mixture was stirred at 90–95 °C for 48 h and then concentrated. EtOAc (10 mL) and 10% HCl (3 mL) were added. The mixture was stirred for 0.5 h, washed (water and brine), and dried. Concentration and crystallization (EtOAc/CH₂Cl₂/hexane) produced 58 mg (72%) of **31** as a white powder, *R_f* 0.27 (50% EtOAc/hexane); mp 235–240 °C. IR (powder) 3377, 2906, 1486, 1256 cm⁻¹; ¹H NMR (C²H₃O²H) δ 1.85 (s, 6H, AdCH₂), 2.08 (s, 3H, AdCH), 2.22 (s, 6H, AdCH₂), 6.83 (d, *J* = 8.1 Hz, 1H, 5'-ArH), 7.18 (dd, *J* = 8.1, 2.1 Hz, 1H, 6'-ArH), 7.29 (d, *J* = 2.4 Hz, 1H, 2'-ArH), 7.57 (d, *J* = 7.8 Hz, 1H, 5-ArH), 8.01 (dd, *J* = 7.8, 1.5 Hz, 1H, 6-ArH), 8.18 ppm (d, *J* = 1.5 Hz, 1H, 2-ArH). FTMS (HRMS) calcd C₂₃H₂₃ClN₄O [M + H]⁺ expected 407.1633, found 407.1630.

Ethyl (E)-4-Benzoyloxy-3-chlorocinnamate (32).^{8,72} To triethyl phosphonoacetate (2.24 g, 10 mmol) in Et₂O (20 mL) stirred under argon in a dry ice-acetone bath was added 0.91 M KN(SiMe₃)₂ (10.0 mmol) in THF (11.0 mL). The mixture was stirred for 0.5 h before 4-benzoyloxy-3-chlorobenzaldehyde (**18**) (2.00 g, 8.1 mmol) in THF (40 mL) was added dropwise over a 0.5-h period, stirred for 1 h more, allowed to warm to room temperature, stirred overnight, poured into water (50 mL) containing HOAc (2 mL), and extracted (Et₂O, 100 mL). The extract was washed (water and brine), dried, and concentrated. Chromatography (EtOAc/hexane) afforded 2.3 g (91%) of **32** as a white solid, *R_f* 0.41 (10% EtOAc/hexane); mp 72–74 °C. IR (CHCl₃) 2961, 1706, 1634, 1508 cm⁻¹; ¹H NMR δ 1.33 (t, *J* = 7.2 Hz, 3H, CH₃), 4.25 (q, *J* = 7.2 Hz, 2H, OCH₂), 5.20 (s, 2H, ArCH₂), 6.31 (d, *J* = 15.9 Hz, 1H, CH=CHCO), 6.95 (d, *J* = 8.7 Hz, 1H, 5-ArH), 7.36–7.45 (m, 6H, 6-ArH, ArH), 7.56 (d, *J* = 16.2 Hz, 1H, CH=CHCO), 7.59 ppm (s, 1H, 2-ArH). This product was debenzylated to **33**.

(E)-4-[3'-(1-Adamantyl)-4'-benzyloxyphenyl]-3-chlorocinnamyl Alcohol (36). To a stirred solution of **35** (264 mg, 0.5 mmol) in CH₂Cl₂ (5 mL) at –78 °C under argon was added 1.5 mL of 1.0 M DIBAL (1.5 mmol) in hexane. The mixture was stirred at –78 °C for 3 h, diluted with 1 N HCl, and then extracted (EtOAc). The extract was washed (water and brine), dried, and concentrated.

Chromatography (10% EtOAc/hexane) gave 220 mg (91%) of **36** as a white powder, *R_f* 0.28 (20% EtOAc/hexane); mp 72–74 °C. IR (CHCl₃) 3399, 2906, 1601 cm⁻¹; ¹H NMR δ 1.73 (s, 6H, AdCH₂), 2.04 (s, 3H, AdCH), 2.17 (s, 6H, AdCH₂), 4.35 (d, *J* = 4.2 Hz, 2H, OCH₂), 5.16 (s, 2H, ArCH₂), 7.64 (td, *J* = 5.4, 16.2 Hz, 1H, CH=CHCH₂OH), 6.61 (d, *J* = 15.2 Hz, 1H, CH=CHCH₂OH), 7.00 (d, *J* = 8.7 Hz, 1H, 5'-ArH), 7.30–7.42 (m, 5H, ArH), 7.40 (d, *J* = 7.5 Hz, 1H, 6'-ArH), 7.42 (s, 1H, 2'-ArH), 7.50 (d, *J* = 8.1 Hz, 2H, 5,6-ArH), 7.53 ppm (s, 1H, 2-ArH). HRMS calcd C₃₂H₃₃ClO₂ [M + Na]⁺ 507.2061, found 507.2066.

(E)-4-[3'-(1-Adamantyl)-4'-benzyloxyphenyl]-3-chlorocinnamaldehyde (37). To a stirred solution of oxalyl chloride (127 mg, 1 mmol) in CH₂Cl₂ (2 mL) at –78 °C under argon was slowly added Me₂SO (156 mg, 2 mmol) in CH₂Cl₂ (1 mL) according to the method of Swern.⁴⁸ The solution was stirred at –78 °C for 10 min, **36** (170 mg, 0.35 mmol) in CH₂Cl₂ (2 mL) was slowly added, and stirring was continued at –78 °C for 20 min before Et₃N (303 mg, 3.0 mmol) was added. The mixture was allowed to warm to room temperature and diluted with CH₂Cl₂ (20 mL). The organic layer was washed (water and brine), dried, and concentrated. Chromatography (5% EtOAc/hexane) gave 122 mg (72%) of **37** as a white powder, mp 56–58 °C. IR (CHCl₃) 2906, 1681, 1602 cm⁻¹; ¹H NMR δ 1.73 (s, 6H, AdCH₂), 2.05 (s, 3H, AdCH), 2.17 (s, 6H, AdCH₂), 5.17 (s, 2H, ArCH₂), 6.73 (dd, *J* = 15.2, 7.5 Hz, 1H, CH=CHCHO), 7.02 (d, *J* = 8.7 Hz, 1H, 5'-ArH), 7.29 (dd, *J* = 8.1, 2.1 Hz, 1H, 6'-ArH), 7.35–7.44 (m, 5H, ArH), 7.41 (d, *J* = 6.9 Hz, 1H, 5-ArH), 7.49 (d, *J* = 6.9 Hz, 1H, 6-ArH), 7.50 (s, 1H, 2'-ArH), 7.51 (d, *J* = 15.9 Hz, 1H, CH=CHCHO), 7.66 (s, 1H, 2-ArH), 9.73 ppm (d, *J* = 7.5 Hz, 1H, CHO). FTMS (HRMS) calcd C₃₂H₃₂ClO₂ [M + H]⁺ expected 501.2200, found 501.2276.

General Procedure for Converting Aldehydes 37 and 41 to 2,4-Thiazolidinediones. To a stirred solution of aldehyde (0.1 mmol) and 2,4-thiazolidinedione (23 mg, 0.2 mmol) in toluene (1 mL) were added NHEt₂ (0.1 mL) and HOAc (0.05 mL). The mixture was stirred at reflux for 2 h, cooled, and diluted with CH₂Cl₂ (10 mL). The organic layer was washed (water and brine) and dried. Concentration and chromatography gave the thiazolidinedione.

5-[3-[3'-(1-Adamantyl)-4'-benzyloxy-2-chloro-4-biphenyl]-(2E)-2-propenylidene]-2,4-thiazolidinedione (38). **37** (46 mg, 0.1 mmol) gave 34 mg (62%) of **38** as a yellow powder, *R_f* 0.31 (30% EtOAc/hexane); mp 212–215 °C. IR (CHCl₃) 3186, 1733, 1692 cm⁻¹; ¹H NMR δ 1.73 (s, 6H, AdCH₂), 2.04 (s, 3H, AdCH), 2.17 (s, 6H, AdCH₂), 5.17 (s, 2H, ArCH₂), 6.70 (dd, *J* = 15.6, 8.7 Hz, 1H, ArCH=CHCH=C), 7.00 (d, *J* = 8.4 Hz, 1H, 5'-ArH), 7.02 (d, *J* = 14.2 Hz, 1H, ArCH=CHCH=C), 7.27–7.46 (m, 7H, 5-ArH, 6'-ArH, Ar), 7.51 (d, *J* = 1.2 Hz, 1H, 2'-ArH), 7.52 (d, *J* = 6.6 Hz, 1H, 6-ArH), 7.54 (d, *J* = 15.1 Hz, 1H, ArCH=CHCH=C), 7.60 (s, 1H, 3-ArH), 8.39 ppm (s, 1H, NH). HRMS calcd C₃₅H₃₂ClNO₃S [M – H][–] 580.1719, found 580.1714.

5-[4-[3'-(1-Adamantyl)-4'-benzyloxyphenyl]-3-chlorobenzylidene]-2,4-thiazolidinedione (42). **41** (46 mg, 0.1 mmol) gave 34 mg (62%) of **42** as a yellow powder, *R_f* (10% EtOAc/hexane); mp 200–203 °C. IR (CHCl₃) 3173, 2904, 1739, 1689 cm⁻¹; ¹H NMR δ 1.74 (s, 6H, AdCH₂), 2.05 (s, 3H, AdCH), 2.18 (d, *J* = 2.4 Hz, 6H, AdCH₂), 5.18 (s, 2H, ArCH₂), 7.02 (d, *J* = 8.4 Hz, 1H, 5'-ArH), 7.30 (dd, *J* = 8.4, 2.1 Hz, 1H, 6'-ArH), 7.35–7.43 (m, 6H, 2'-ArH, ArH), 7.48 (d, *J* = 7.8 Hz, 1H, 6-ArH), 7.52 (d, *J* = 6.6 Hz, 1H, 5-ArH), 7.60 (d, *J* = 7.8 Hz, 1H, 2-ArH), 7.81 (s, 1H, ArCH=C), 8.14 ppm (bs, 1H, NH). HRMS calcd C₃₃H₃₀ClNO₃S [M – H][–] 554.1562, found 554.1552.

2-[[3'-(1-Adamantyl)-4'-benzyloxy-2-chloro-4-biphenyl]-methylene]propanedinitrile (44). A reported procedure⁴⁹ was adapted. A mixture of **41** (102 mg, 0.22 mmol) and malononitrile (18 mg, 0.27 mmol) in anhydrous DMF (0.6 mL) was stirred in a 103 °C oil-bath for 7 h, cooled to room temperature, and diluted with H₂O (8 mL) and EtOAc (80 mL). The organic layer was washed (brine) and dried. The residue obtained on concentration was purified by chromatography (9% EtOAc/hexane) to give 78 mg (70%) of **44** as a yellow solid, mp 170–171 °C, which was deprotected to give **45**. ¹H NMR δ 1.76 (bs, 6H, AdCH₂), 2.08 (bs, 3H, AdCH), 2.20 (bs, 6H, AdCH₂), 5.20 (s, 2H, ArCH₂), 7.05

(d, $J = 8.4$ Hz, 1H, 5'-ArH), 7.32–7.57 (m, 8H, 5-ArH, 2'-ArH, 6'-ArH, ArH), 7.74 (s, 1H, $\text{CH}=\text{C}(\text{CN})_2$), 7.92–7.96 ppm (m, 2H, 3-ArH, 6-ArH).

(E)-4-[3'-(1-Adamantyl)-4'-benzyloxyphenyl]-3-chlorocinnamic Acid (46).⁵ A mixture of **35** (174 mg, 0.34 mmol) and LiOH·H₂O (47 mg, 3.3 mmol) in CH₃OH/THF/H₂O (0.6:1.6:0.55) was stirred for 6 h. After removal of solvent, the residue suspended in H₂O (7 mL) and 2 N HCl (5 mL) was extracted with EtOAc (100 mL). The organic layer was washed (brine) and dried. Removal of solvent gave 157 mg (93%) of **46** as a pale-tan solid, which was used directly in the next step. ¹H NMR δ 1.74 (bs, 6H, AdCH₂), 2.05 (bs, 3H, AdCH), 2.19 (bs, 6H, AdCH₂), 5.18 (s, 2H, ArCH₂), 6.48 (d, $J = 15$ Hz, 1H, $\text{CH}=\text{CHCO}$), 7.01 (m, 1H, 5'-ArH), 7.28–7.55 (m, 9H, 6'-ArH, 2-ArH, 5-ArH, 6-ArH, ArH), 7.66 (s, 1H, 2'-ArH), 7.75 ppm (d, $J = 15$ Hz, 1H, $\text{CH}=\text{CHCO}$).

N-(Tetrahydro-2H-pyran-2-yloxy) (E)-4-[3'-(1-Adamantyl)-4'-benzyloxyphenyl]-3-chlorocinnamic Acid (47). A reported procedure⁵⁰ was followed. To a stirred solution of **46** (102 mg, 0.205 mmol) in CHCl₃ (4 mL) at 0 °C (ice-bath) were added DMAP (47 mg, 0.39 mmol) and *O*-(tetrahydro-2H-pyran-2-yl)hydroxylamine (36 mg, 0.31 mmol). Stirring was continued at 0 °C for 20 min more, before DIC (48 μ L, 0.31 mmol) was added. After 1 h, the mixture was warmed to room temperature, stirred for 48 h, quenched with saturated NH₄Cl (8 mL), and extracted with EtOAc (90 mL). The extract was washed (sat. NH₄Cl and brine) and dried. Solvent was removed at reduced pressure and the residue chromatographed (33% EtOAc/hexane) to give 56 mg (46%) of **47** as a pale-tan solid, 91–93 °C. ¹H NMR δ 1.64 (m, 4H, 4-THPH, 5-THPH), 1.74 (bs, 6H AdCH₂), 1.87 (m, 2H, 3-THPH), 2.06 (bs, 3H, AdCH), 2.18 (bs, 6H, AdCH₂), 3.64 (m, 1H, 6-THPH), 3.98 (m, 1H, 6-THPH), 5.06 (bs, 1H, 2-THPH), 5.18 (s, 2H, ArCH₂), 7.01 (d, $J = 8.1$ Hz, 1H, 5'-ArH), 7.29 (dd, $J = 8.4$, 1.5 Hz, 1H, 6'-ArH), 7.33–7.46 (m, 7H, $\text{CH}=\text{CHCO}$, 5-ArH, ArH), 7.51–7.63 (m, 3H, 2-ArH, 6-ArH, 2'-ArH), 7.72 ppm (d, $J = 15.3$ Hz, 1H, $\text{CH}=\text{CHCO}$).

3'-(1-Adamantyl)-4'-benzyloxyphenyl-3-chloroaniline (52). A mixture of **51** (2.08 g, 4.4 mmol) and SnCl₂·2H₂O (4.96 g, 44 mmol) in EtOH (20 mL) was heated at 88 °C (oil-bath) for 2.5 h, cooled to room temperature, diluted with H₂O (10 mL), and adjusted to pH 7–8 by addition of 2 N NaOH (21 mL) and 5% NaHCO₃ (19 mL). This mixture was stirred for 1 h and extracted (3 \times 350 mL EtOAc). The organic layer was washed (sat. brine) and dried. The concentrated residue was chromatographed (28% EtOAc/hexane) to give 1.766 g (90%) of **52** as a white solid, mp 154–155 °C. IR 3391, 2905, 1189 cm⁻¹; ¹H NMR δ 1.73 (m, 6H, AdCH₂), 2.05 (m, 3H, AdCH), 2.18 (m, 6H, AdCH₂), 3.73 (bs, 2H, NH₂), 5.16 (s, 2H, ArCH₂), 6.62 (dd, $J = 8.1$, 2.4 Hz, 1H, 5-ArH), 6.8 (d, $J = 2.4$ Hz, 1H, 2-ArH), 6.97 (d, $J = 8.1$ Hz, 1H, 6-ArH), 7.15 (d, $J = 8.4$ Hz, 1H, 5'-ArH), 7.35 (dd, $J = 8.4$, 2.4 Hz, 1H, 6'-ArH), 7.32 (d, $J = 8.4$ Hz, 1H, 2'-ArH), 7.33–7.55 ppm (m, 5H, ArH). HRMS calcd C₂₉H₃₀ClNO [M + H]⁺ 444.2089, found 444.2096.

3'-(1-Adamantyl)-4'-benzyloxy-4-bromo-2-chlorobiphenyl (53). To CuBr₂ (1.19 g, 5.32 mmol) and *tert*-butyl nitrite (899 μ L, 6.81 mmol) in anhydrous MeCN (5 mL) at 0 °C were slowly added under argon **52** (1.89 g, 4.25 mmol) and MeCN (11 mL), and stirring was continued for 30 min. The mixture was warmed to room temperature, stirred for 2 h, at which time no insoluble **52** remained, quenched with 2 N HCl (100 mL), and extracted (3 \times 300 mL Et₂O). The organic layer was washed (sat. brine) and dried. After concentration, the residue was chromatographed (hexane) to give 973 mg (45%) of **53** as a pale-yellow solid, mp 58–60 °C. IR 2902, 1220 cm⁻¹; ¹H NMR δ 1.74 (bs, 6H, AdCH₂), 2.05 (bs, 3H, AdCH), 2.18 (m, 6H, AdCH₂), 5.17 (s, 2H, ArCH₂), 7.01 (d, $J = 8.1$ Hz, 1H, 5'-ArH), 7.23 (d, $J = 8.4$ Hz, 1H, 6-ArH), 7.25 (dd, $J = 8.4$, 2.1 Hz, 1H, 6'-ArH), 7.32 (d, $J = 2.1$ Hz, 1H, 2'-ArH), 7.33–7.55 (m, 6H, 5-ArH, ArH), 7.64 ppm (d, $J = 2.1$ Hz, 1H, 3-ArH). HRMS calcd C₂₉H₂₈BrClO [M + H]⁺ 507.1085, found 507.1068.

3'-(1-Adamantyl)-4'-benzyloxy-2-chloro-4-(2-trimethylsilylethynyl)biphenyl (54). A reported procedure⁵² was adapted. A mixture

of **53** (340 mg, 0.67 mmol), trimethylsilylacetylene (186 μ L, 1.34 mmol), Pd(PPh₃)₄ (92 mg, 0.08 mmol), and CuI (5 mg, 0.026 mmol) was heated at 102 °C (oil-bath) under argon for 3.5 h, cooled to room temperature, diluted with EtOAc (90 mL), and filtered through silica gel. The filtrate was concentrated, and the residue was chromatographed (1% EtOAc/hexane) to give 350 mg (99%) of **54** as a pale-yellow solid, mp 55–57 °C. IR 2902, 2221, 1286 cm⁻¹; ¹H NMR δ 0.27 (s, 9H, Si(CH₃)₃), 1.74 (bs, 6H, AdCH₂), 2.05 (bs, 3H, AdCH), 2.18 (m, 6H, AdCH₂), 5.17 (s, 2H, ArCH₂), 7.01 (d, $J = 8.7$ Hz, 1H, 5'-ArH), 7.27 (dd, $J = 8.7$, 2.1 Hz, 1H, 6'-ArH), 7.29 (d, $J = 8.4$ Hz, 1H, 6-ArH), 7.30–7.46 (m, 6H, 2'-ArH, ArH), 7.53 (dd, $J = 8.4$, 1.5 Hz, 1H, 5-ArH), 7.58 ppm (d, $J = 1.5$ Hz, 1H, 3-ArH). HRMS calcd C₃₄H₃₇ClSiO [M + H]⁺ 525.2375, found 525.2379.

3'-(1-Adamantyl)-4'-benzyloxy-2-chloro-4-ethynylbiphenyl (55). To a solution of **54** (350 mg, 0.67 mmol) in THF (15 mL) was added 0.9 mL of 1.0 M (*n*-Bu)₄NF (0.88 mmol) in THF. The mixture was stirred for 1 h, diluted with H₂O (20 mL), and extracted with EtOAc (3 \times 200 mL). The extract was washed (sat. brine) and dried. After concentration, the residue was chromatographed (1% EtOAc/hexane) to give 295 mg (96%) of **55** as a white solid, mp 94–96 °C. ¹H NMR δ 1.74 (bs, 6H, AdCH₂), 2.06 (bs, 3H, AdCH), 2.18 (m, 6H, AdCH₂), 3.14 (s, 1H, C \equiv CH), 5.17 (s, 2H, ArCH₂), 7.01 (d, $J = 8.4$ Hz, 1H, 5'-ArH), 7.28 (dd, $J = 8.1$, 2.4 Hz, 1H, 6'-ArH), 7.31 (d, $J = 8.1$ Hz, 1H, 6-ArH), 7.35 (d, $J = 2.4$ Hz, 1H, 2'-ArH), 7.32–7.55 (m, 6H, 5-ArH, ArH), 7.6 ppm (d, $J = 1.5$ Hz, 1H, 3-ArH). HRMS calcd C₃₁H₂₉ClO [M + H]⁺ 453.1980, found 453.1978.

(E)-2-[3'-(1-Adamantyl)-4'-benzyloxy-2-chloro-4-biphenyl]ethenyl-1,3,2-benzodioxaborole (56). The procedure of Brown et al.⁵³ was adapted. A mixture of **55** (295 mg, 0.65 mmol) and 0.67 mL of 1.0 M catecholborane (0.67 mmol) in THF was stirred under argon at 91 °C (oil-bath) for 5 h, cooled to room temperature, and diluted with THF (3 mL) for transfer. After concentration, the residue was chromatographed (1% to 40% EtOAc/hexane) to give 59 mg (26%) of **56** as a pale-yellow solid, mp 158–161 °C. ¹H NMR δ 1.75 (bs, 6H, AdCH₂), 2.07 (bs, 3H, AdCH), 2.21 (m, 6H, AdCH₂), 5.19 (s, 2H, ArCH₂), 6.42 (d, $J = 18$ Hz, 1H, $\text{CH}=\text{CHB}$), 7.01–7.07 (m, 3H, ArH), 7.27–7.49 (m, 8H, ArH), 7.52–7.60 (m, 3H, ArH), 7.75 (s, 1H, ArH), 7.79 ppm (d, $J = 18$ Hz, 1H, $\text{CH}=\text{CHB}$).

(3E)-4-[3'-(1-Adamantyl)-4'-benzyloxy-2-chloro-4-biphenyl]but-3-en-2-one (58). A reported procedure⁵⁴ was modified. A mixture of 4-[3'-(1-Adamantyl)-4'-benzyloxyphenyl]-3-chlorobenzaldehyde (**41**) (303 mg, 0.66 mmol), (2-oxopropyl)triphenylphosphonium bromide (397 mg, 0.99 mmol) and 1,5,7-triazabicyclo[4.4.0]dec-5-ene (157 mg, 1.13 mmol) in THF (3 mL) was stirred for 23 h at room temperature and then at 70 °C for 2 h. The mixture was cooled to room temperature and diluted with H₂O (10 mL) and EtOAc (150 mL). The organic layer was washed (sat. brine) and dried. The residue obtained on concentration was chromatographed (12% EtOAc/hexane) to give 124 mg (38%) of **58** as a yellow wax, mp 73–75 °C. IR 2902, 2849, 1683 cm⁻¹; ¹H NMR δ 1.74 (bs, 6H, AdCH₂), 2.06 (bs, 3H, AdCH), 2.19 (bs, 6H, AdCH₂), 2.42 (s, 3H, CH₃CO), 5.18 (s, 2H, ArCH₂), 6.75 (d, $J = 16.2$ Hz, 1H, $\text{CH}=\text{CHCO}$), 7.02 (d, $J = 8.4$ Hz, 1H, 5'-ArH), 7.30 (dd, $J = 8.4$, 2.1 Hz, 1H, 6'-ArH), 7.34–7.56 (m, 9H, 2'-ArH, 5-ArH, 6-ArH, $\text{CH}=\text{CHCO}$, ArH), 7.66 ppm (d, $J = 1.2$ Hz, 1H, 3-ArH). HRMS calcd C₃₃H₃₃ClO₂ [M + H]⁺ 497.2242, found 497.2240.

(3E)-4-[3'-(1-Adamantyl)-4'-benzyloxy-2-chloro-4-biphenyl]-2-oxobut-3-enal (59). A reported procedure⁵⁵ was applied. A mixture of **58** (124 mg, 0.25 mmol) and H₂SeO₃ (35 mg, 0.27 mmol) in 1.0 mL of dioxane and 0.1 mL of H₂O was heated at reflux for 1.5 h under argon, cooled to room temperature, and diluted with EtOAc (120 mL). The organic layer was washed (sat. brine) and dried. The residue obtained on concentration was chromatographed (33% EtOAc/hexane) to give 35 mg (27%) of **59** as a yellow wax, mp 84–86 °C. IR 2904, 2853, 1713, 1690 cm⁻¹; ¹H NMR δ 1.74 (bs, 6H, AdCH₂), 2.06 (bs, 3H, AdCH), 2.19 (bs, 6H, AdCH₂), 5.18 (s, 2H, ArCH₂), 6.93 (d, $J = 16.2$ Hz, 1H, $\text{CH}=\text{CHCO}$), 7.02 (dd, $J = 8.1$, 2.1 Hz, 1H, 6'-ArH), 7.28–7.56 (m, 9H, 5-ArH, 6-ArH,

2'-ArH, 5'-ArH, ArH), 7.76 (d, $J = 1.5$ Hz, 1H, 3-ArH), 7.97 (d, $J = 16.2$ Hz, 1H, CH=CHCO), 9.47 ppm (s, 1H, CHO). HRMS calcd $C_{33}H_{31}ClO_3$ [M + H]⁺ 511.2034, found 511.2038.

Diethyl (E)-2-[3'-(1-Adamantyl)-4'-benzyloxy-2-chloro-4-biphenyl]ethenylphosphonate (61). A reported method⁵⁶ was modified. To a solution of **41** (0.14 mmol, 65 mg) and tetraethyl methylenebisphosphonate (0.14 mmol, 36 μ L) in CH_2Cl_2 (0.8 mL) was added 50% aq NaOH (0.8 mL). The mixture was stirred for 10 min, diluted with H_2O (8 mL), and extracted (60 mL EtOAc). The extract was washed (2 N HCl and brine) and dried. The residue obtained on concentration was purified by chromatography (50% to 60% EtOAc/hexane) to give 82 mg (98%) of **61** as a colorless gel. ¹H NMR δ 1.40 (t, $J = 6.9$ Hz, 6H, OCH_2CH_3), 1.76 (bs, 6H, $AdCH_2$), 2.07 (bs, 3H, $AdCH$), 2.20 (bs, 6H, $AdCH_2$), 4.18 (m, 4H, OCH_2CH_3), 5.20 (s, 2H, $ArCH_2$), 6.32 (t, $J = 17.4$ Hz, 1H, CH=CHP), 7.03 (d, $J = 8.1$ Hz, 1H, 5'-ArH), 7.31 (dd, $J = 8.1$, 2.1 Hz, 1H, 6'-ArH), 7.28–7.57 (m, 9 H, 2'-ArH, 5-ArH, 6-ArH, ArH, CH=CHP), 7.64 (s, 1H, 3-ArH). HRMS calcd $C_{35}H_{40}ClO_4P$ [M + H]⁺ 591.2425, found 591.2429.

(E)-2-[3'-(1-Adamantyl)-2-chloro-4'-hydroxy-4-biphenyl]ethenylphosphonic Acid Monoethyl Ester (63). A literature method⁵⁷ was adapted. A suspension of **62** (0.12 mmol, 61 mg) in aq 20% HCl (5 mL) was heated at reflux under argon for 6 h. After removal of some water at reduced pressure from the resultant solution, the residue was extracted (3 \times 40 mL EtOAc). The organic extract was washed (brine) and dried. The residue obtained on concentration was chromatographed (EtOAc/hexane/MeOH, 2:2:1, to EtOAc/MeOH/HOAc, 5:3:0.01) to give 45 mg (80%) of **63** as an off-white solid, mp 260 $^{\circ}C$ (dec). IR 3328, 2902, 1617, 1603, 1035 cm^{-1} ; ¹H NMR δ 1.27 (t, $J = 6.9$ Hz, 3H, OCH_2CH_3), 1.81 (bs, 6H, $AdCH_2$), 2.05 (bs, 3H, $AdCH$), 2.17 (bs, 6H, $AdCH_2$), 3.93 (m, $J = 6.9$ Hz, 2H, OCH_2CH_3), 6.46 (dd, $J = 17.4$, 15.0 Hz, 1H, CH=CHP), 6.76 (d, $J = 7.8$ Hz, 1H, 5'-ArH), 7.06 (dd, $J = 7.8$, 2.1 Hz, 1H, 6'-ArH), 7.18 (d, $J = 2.1$ Hz, 1H, 2'-ArH), 7.23 (dd, $J = 17.4$, 15.0 Hz, 1H, CH=CHP), 7.29 (d, $J = 7.8$ Hz, 1H, 6-ArH), 7.43 (d, $J = 7.8$ Hz, 1H, 5-ArH), 7.57 ppm (s, 1H, 3-ArH). HRMS calcd $C_{26}H_{30}ClO_4P$ [M - H]⁻ 471.1492, found 471.1487.

Computational Studies. Conformational libraries were prepared for a training set of 55 AHPN (**1**) analogues including 24 active analogues using 30 $^{\circ}$ increment grid rotations for all rotatable bonds employing the CHARMM forcefield in Accelerlys Quanta, a continuum dielectric constant of 80 and no potential truncation for correlation with their apoptotic activity at 1.0 μ M against MDA-MB-231 breast cancer cells after treatment for 96 h. Most of the analogues had a carboxylate moiety and a hydroxyl group adjacent to a bulky hydrophobic group as in AHPN (**1** in Figure 1) and variable hydrophobic groups and ring systems. While not all of the analogues with these features were apoptosis inducers, these moieties appeared to be core-recognition elements inasmuch as their removal eliminated apoptotic activity. An initial pharmacophore/overlap rule was developed using the in-house program MOLMOD,^{74,75} which took as input trial pharmacophore hypotheses in the form of (i) either ligand or 'receptor-based' sites of hydrogen-bond acceptors/donors, hydrophobic moieties, centroids, or user-defined criteria; (ii) an energy window for the low-energy conformations to employ in pharmacophore testing; and (iii) a distance criterion (cutoff) for pharmacophoric distances in order to determine whether a conformation of each ligand had a 3D-distance matrix between the pharmacophore points in common with at least one conformation of each of the other ligands in the training set. Any pharmacophore found within the energy and distance criteria was reported along with all conformers of each analogue complying with the pharmacophore. The program also output a superposition of the analogues at their pharmacophore points for use in 3D-QSAR. Following development of the initial apoptosis pharmacophore for these compounds, the properties of all analogues in their conformations complying with the pharmacophore definition were evaluated using a combination of semiempirical quantum mechanics, a MOPAC-7 AM1 Hamiltonian,⁷⁶ density functional theory as incorporated in Gaussian⁷⁷ and Jaguar (Schrödinger, Portland, OR), and the comparative molecular similarity index analysis (CoMSIA)

field descriptors employed in Tripos QSAR (St. Louis, MO). The validity of the MOLMOD pharmacophore developed from the training set was assessed by using the overlap rule in 3DQSAR (CoMSIA). Models predictive of the percentage of apoptosis of MDA-MB-231 breast cancer cells were developed and used to predict the percentage of apoptosis of MDA-MB-231 breast cancer cells of analogues not included in building the CoMSIA models. A fragment QSAR model was constructed using the isosteric polar/H-bond acceptor replacements shown in Table 3 for the 3-Cl-AHPC carboxyl group. In an effort to understand the SAR of these substitutions we computed: (i) frontier orbital energetics, (ii) Sterimol parameters, (iii) group hydrophobicities, (iv) volumes, (v) areas, (vi) solvent-accessible surface areas, (vii) polar and nonpolar volumes, (viii) globularities, (ix) electrostatic potentials on the van der Waals surface using MOPAC-AM1-derived properties developed by the in-house program GRAPHA and (x) solvation energies and raw pK_a values using density functional theory evaluation. The raw pK_a values were computed from unscaled/uncorrected gas-phase protonation energies.⁵⁸ Combinations of 19 properties were used in several SAR models to interrogate the data for 50% proliferation inhibition (IC₅₀ value) of KG-1, H292, MDA-MB-231, and Du-145 cancer cells in terms of fundamental changes in the polar region. We were able to obtain predictive models for all of the data sets. **Biology. Cell Growth.** Cancer cell lines were obtained from ATCC (Manassas, VA) and grown in DMEM (MDA-MB-231 breast cancer) or RPMI-1640 medium (H292 lung cancer and Du-145 prostate cancer) containing 10% fetal bovine serum (FBS; Tissue Culture Biologicals, Tulare, CA) at 37 $^{\circ}C$ under 6% CO₂. MDA-MB-231 cells were also grown and cultured in DMEM/F-12 medium supplemented with 5% heat-inactivated FBS, as we have previously described.⁶ KG-1 cells were obtained from Dr. H. Phillip Koeffler (UCLA, Cedars-Sinai Medical Center, Los Angeles, CA) and were grown in RPMI-1640 medium supplemented with 5% heat-inactivated FBS and gentamycin (10 μ g/mL). Retinoid-resistant HL-60R leukemia cells were obtained from Dr. Steve Collins (University of Washington, Seattle) and grown under the same conditions.

Cryopreserved, pooled primary human microvascular endothelial (HMVE) cells (Clonetics, San Diego, CA) were grown in endothelial cell growth medium EGM-MV (Clonetics) or in MEV growth medium containing 5% fetal calf serum plus the growth factors and antimicrobials in the accompanying kit (Clonetics). Human dermal microvascular endothelial (HMVE) cells (Cambrex Bioscience, Walkersville, MD) were grown and maintained in EGM-MV medium (Cambrex).

Growth Inhibition. Cells (4×10^3 /well in 96-well plates for MDA-MB-231 or 2×10^3 /well for H292 and Du-145) were allowed to attach for 24 h and then treated for 72 h with each analogue dissolved in Me₂SO or Me₂SO alone (0.1% Me₂SO final concentration). Media and compounds were replaced after 48 h. The number of viable cells was determined using the 3-(4,5-dimethylthiazol-2-yl)-5-(3-carboxymethoxyphenyl)-2-(4-sulfophenyl)-2H-tetrazolium inner salt (MTS) reduction assay (Cell Titer 96 Aqueous Non-radioactive Cell Proliferation Assay, Promega, Madison, WI). Three replicates were done at each concentration.

KG-1, HL-60R, and MDA-MB-231 cells were seeded in six-well plates containing 3 mL of media plus 5% FBS per well and incubated overnight. Compounds were then added in Me₂SO (0.1% final Me₂SO concentration), and cells were incubated at various concentrations for the cited times and harvested. Cell numbers were determined using a hemocytometer for counting as we described.⁶ HMVE cells (3×10^3 in 200- μ L medium/well in 96-well plates) were allowed to attach for 24 h. Compounds dissolved in Me₂SO were added to give 100, 125, 250, and 500-nM final concentrations (final Me₂SO concentration $\leq 0.1\%$). Medium and test compound were replaced every 48 h. After 7 days of treatment, cell growth was determined by Alamar blue staining (BioSource, Camarillo, CA) and measuring emission at 590 nm after excitation at 530 nm by using a fluorimeter (Cytoflor, ABI, Foster City, CA). Results shown in Table 2 are averages of five replicates. HMVE cells (1×10^4 in 1.0 mL of EGM-MV medium/well) were plated into 24-

well plates and incubated for 1 h at 37 °C. Compounds in Me₂SO or Me₂SO alone (0.5% final concentration) were added. After 72-h incubation at 37 °C, cells were detached using trypsin/EDTA and counted using a hemocytometer. Three replicates were performed for the experiments shown in Figure 6.

Cell Apoptosis. KG-1 and HL-60R leukemia and MDA-MB-231 breast cancer cells were seeded and incubated as described in the growth inhibition experiments. Apoptotic cells were identified using acridine orange staining as we have described.⁶

HMVE cells (6×10^4 /well) were seeded in EGM-MV medium into 24-well plates. After a 6-h incubation at 37 °C, cells were further incubated with medium containing various concentrations of 3-Cl-AHPC or 1.0 μ M doxorubicin (Sigma, St. Louis, MO) in Me₂SO, or Me₂SO alone (control) (0.5% final Me₂SO concentration) for 20 h more. Cells were lysed, lysates were centrifuged, and the supernate was analyzed for cytoplasmic histone-associated DNA fragments indicative of apoptosis-induced DNA laddering using the Cell Death Detection ELISA^{PLUS} kit (Roche Diagnostics, Indianapolis, IN) according to the manufacturer's protocol and a microtiter plate reader (Fisher Scientific, Pittsburgh, PA). Experiments were done in triplicate. This protocol was used to obtain data shown in Figure 7.

HMVE Cell Migration. Migration was assayed using 6.5-mm Transwell Chambers having 8 μ m-diameter pores (Corning Costar, Cambridge, MA). Their membrane undersides were coated overnight at 4 °C with Matrigel (Becton Dickinson Labware, Bedford, MA) (30 μ g/mL) in EBM medium. Chambers were blocked for 2 h with a solution of 1% bovine serum albumin in phosphate-buffered saline, pH 7.2, and then transferred to wells in 24-well plates filled with EGM-MV medium (500 μ L/well). HMVE cells (80% confluent) were released with enzyme-free cell dissociation buffer (Gibco, Long Island, NY), washed, and resuspended in medium containing 3-Cl-AHPC (**5**) (0.05, 0.5, 5.0, 50, and 500 nM final concentration) in Me₂SO or Me₂SO alone (0.01% final Me₂SO concentration). Cells (40×10^4 /well) in 200 μ L of medium were placed in the Transwells, and migration to the underside of the precoated filter was examined after 5-h incubation at 37 °C. Membranes were fixed and stained with Diff-Quick (Dade Diagnostics, Aguada, PR). Three high-power microscope fields were counted in each replicate well, and results were expressed as mean number of cells per field \pm SD of three replicates.

HMVE Tubule Formation. Tube formation was assayed as described by Nangia-Makker et al.⁷⁸ with some modification. Matrigel (100 μ L) liquified on ice was added to 96-well plates and then heated at 37 °C for 1 h to induce gelation. Trypsinized HMVE cells (5×10^4 in 150 μ L EGM-MV medium/well) were plated in each well. After a 1-h incubation at 37 °C, cells were incubated at 37 °C with 0.25 μ M or 1.0 μ M 3-Cl-AHPC (**5**) in Me₂SO or Me₂SO alone (0.05% final concentration) for 18 h. Tubule formation was assessed using an Optiphot microscope (Nikon, Melville, KN) attached to a camera (Coolsnap Pro) having 1392 \times 1040 resolution (Media Cybernetics, Silver Spring, MD). Phase-contrast images were captured using Image-Pro Express software (Media Cybernetics) and a PlanApo 10 \times objective (Nikon) with a 0.5 numerical aperture. Total tube length was determined using NIH Image software (NIMH, Rockville, MD). Four random fields were measured for each well of three replicates.

Inhibition of PTP Activity. The phosphatase-catalyzed hydrolysis of 6,8-difluoro-4-methylumbelliferyl phosphate (Invitrogen, Carlsbad, CA) in the presence of each compound in Me₂SO or Me₂SO alone (5% final concentration) was assayed at 30 °C in 60 μ L of 0.15 M Bis-Tris buffer, pH 6.0, having 150-mM ionic strength (adjusted with NaCl) and containing 1.0 mM dithiothreitol per well in 96-well plates. SHP-2 (gift of Dr. Gen-Sheng Feng, Burnham Institute) was at 5 nM and CD45 (BioMol, Plymouth Meeting, PA) at 1 nM. Compounds were assayed at 0, 0.032, 0.16, 0.8, 4.0, 20.0, 100, and 500 μ M. The initial reaction rate at a fixed substrate concentration, which was equal to the corresponding K_m value of 100 μ M for SHP-2 and CD45, was determined by measuring the 460-nm emission after excitation of the fluorescent cleavage product, 6,8-difluoro-7-hydroxy-4-methylcoumarin, at 360 nm using

a FLx800 microplate reader (Bio-Tek Instruments, Winooski, VT). Nonenzymatic hydrolysis of the substrate was corrected by measuring the Me₂SO control without enzyme. IC₅₀ values were determined by plotting the relative activity versus inhibitor concentration using Prism software (GraphPad Software, San Diego, CA) and fitting to the equation $V_i/V_0 = IC_{50}/(IC_{50} + [I])$, where V_i was reaction velocity at inhibitor concentration [I], V_0 was the reaction velocity without inhibitor and $IC_{50} = K_i + K_i[S]/K_m$, where K_i was the dissociation constant for binding of inhibitor to enzyme, [S] was the substrate concentration, and K_m was the Michaelis–Menten constant.

Assay for NR4A1 Expression by Western Blotting. MDA-MB-231, H292, and DU145 cells were grown for 24 h in medium containing 10% FBS and then treated with 1.0 μ M 3-Cl-AHPC (**5**) for 3 or 6 h. Cell lysates were prepared and boiled in sodium dodecyl sulfate (SDS) sample buffer and resolved by SDS–8% polyacrylamide gel electrophoresis. PAGE-separated proteins were transferred to nitrocellulose membranes, which were then blocked in 5% milk in TBST buffer (10 mM Tris-HCl, pH 8.0, containing 150 mM NaCl and 0.05% Tween 20) for 30 min, incubated with monoclonal anti-NGFI-B (rat NR4A1) antibody (1:1000 dilution) (R&D, Minneapolis, MN) in 5% milk in TBST for 2 h at room temperature, washed (3 \times TBST), incubated in TBST containing horseradish peroxidase-linked anti-mouse immunoglobulin G for 1 h at room temperature, and washed (3 \times TBST). Immunoreactive products were detected by chemiluminescence using an enhanced chemiluminescence system (Amersham, Piscataway, NJ).

Receptor Binding Assay. Expression of recombinant glutathione S-transferase (GST)–human SHP chimeric protein (GST–SHP), cell lysis, isolation of GST–SHP using glutathione-Sepharose beads, incubation of beads with [5,5'-³H₂]AHPN⁴² in the presence or absence of 3-Cl-AHPC (**5**), an analogue, or vehicle alone, and separation of bound from nonbound label were performed as we described.¹⁴ Briefly, to GST–SHP (150–500 ng)-bound beads was added nonlabeled **5** or an analogue at a final concentration of 50 μ M in binding buffer (0.4 mL). This mixture was incubated on ice for 45 min before [5,5'-³H₂]AHPN (5-nM final concentration) was added. Incubation was continued for 2 h at 4 °C. Beads were then washed (binding buffer) and either added directly to the scintillation liquid or eluted with 50 mM sodium bicarbonate and 1% sodium dodecyl sulfate and the eluate added to scintillation fluid. Both methods gave similar results.

Acknowledgment. We are grateful for support of this research by the following grants P01 CA51993 (M.I.D., J.A.F., X.-K. Z.), R01 CA109370 (M.I.D., J.A.F.), California Breast Cancer Research Program Grant 6XB-0018 (M.I.D., D.L.H., G.H.L.) and California Tobacco-Related Diseases Research Grant 11RT-0081 (M.I.D., X.-K. Z.).

Supporting Information Available: Tables S1 and S2 showing data and calculations illustrated by graph in Figure 4, Table S3 listing HPLC analyses of target compounds using two different solvent systems, and Table S4 listing data on competitive inhibition of binding to SHP. This material is available free of charge via the Internet at <http://pubs.acs.org>.

References

- Bernard, B. A.; Bernardon, J. M.; Delescluse, C.; Martin, B.; Lenoir, M. C.; Maignan, J.; Charpentier, B.; Pilgrim, W. R.; Reichert, U.; Shroot, B. Identification of synthetic retinoids with selectivity for human nuclear retinoic acid receptor gamma. *Biochem. Biophys. Res. Commun.* **1992**, *186*, 977–983.
- Charpentier, B.; Bernardon, J. M.; Eustache, J.; Millois, C.; Martin, B.; Michel, S.; Shroot, B. Synthesis, structure-affinity relationships, and biological activities of ligands binding to retinoic acid receptor subtypes. *J. Med. Chem.* **1995**, *38*, 4993–5006.
- Shao, Z. M.; Dawson, M. I.; Li, X. S.; Rishi, A. K.; Sheikh, M. S.; Han, Q. X.; Ordonez, J. V.; Shroot, B.; Fontana, J. A. p53 independent G₀/G₁ arrest and apoptosis induced by a novel retinoid in human breast cancer cells. *Oncogene* **1995**, *11*, 493–504.

- (4) Li, X. S.; Rishi, A. K.; Shao, Z. M.; Dawson, M. I.; Jong, L.; Shroot, B.; Reichert, U.; Ordonez, J.; Fontana, J. A. Posttranscriptional regulation of p21^{WAF1/CIP1} expression in human breast carcinoma cells. *Cancer Res.* **1996**, *56*, 5055–5062.
- (5) Zhang, Y.; Dawson, M. I.; Mohammad, R.; Rishi, A. K.; Farhana, L.; Feng, K. C.; Leid, M.; Peterson, V. J.; Zhang, X. K.; Edelstein, M.; Eilander, D.; Biggar, S.; Wall, N.; Reichert, U.; Fontana, J. A. Induction of apoptosis of human B-CLL and ALL cells by a novel retinoid and its nonretinoid analog. *Blood* **2002**, *100*, 2917–2925.
- (6) Dawson, M. I.; Harris, D. L.; Liu, G.; Hobbs, P. D.; Lange, C. W.; Jong, L.; Bruey-Sedano, N.; James, S. Y.; Zhang, X. K.; Peterson, V. J.; Leid, M.; Farhana, L.; Rishi, A. K.; Fontana, J. A. Antagonist analogue of 6-[3'-(1-adamantyl)-4'-hydroxyphenyl]-2-naphthalene-carboxylic acid (AHPN) family of apoptosis inducers that effectively blocks AHPN-induced apoptosis but not cell-cycle arrest. *J. Med. Chem.* **2004**, *47*, 3518–3536.
- (7) Farhana, L.; Dawson, M. I.; Fontana, J. A. Apoptosis induction by a novel retinoid-related molecule requires nuclear factor- κ B activation. *Cancer Res.* **2005**, *65*, 4909–4917.
- (8) Zhang, Y.; Dawson, M. I.; Ning, Y.; Polin, L.; Parchment, R. E.; Corbett, T.; Mohamed, A. N.; Feng, K. C.; Farhana, L.; Rishi, A. K.; Hogge, D.; Leid, M.; Peterson, V. J.; Zhang, X. K.; Mohammad, R.; Lu, J. S.; Willman, C.; VanBuren, E.; Biggar, S.; Edelstein, M.; Eilander, D.; Fontana, J. A. Induction of apoptosis in retinoid-refractory acute myelogenous leukemia by a novel AHPN analog. *Blood* **2003**, *102*, 3743–3752.
- (9) Han, Y. H.; Cao, X.; Lin, B.; Lin, F.; Kolluri, S. K.; Stebbins, J.; Reed, J. C.; Dawson, M. I.; Zhang, X.-K. Regulation of Nur77 nuclear export by c-Jun N-terminal kinase and Akt. *Oncogene* **2006**, *25*, 2974–2986.
- (10) Widschwendter, M.; Berger, J.; Muller, H. M.; Zeimet, A. G.; Marth, C. Epigenetic downregulation of the retinoic acid receptor-beta2 gene in breast cancer. *J. Mammary Gland Biol. Neoplasia* **2001**, *6*, 193–201.
- (11) Lotan, R. Retinoids and their receptors in modulation of differentiation, development, and prevention of head and neck cancers. *Anticancer Res.* **1996**, *16*, 2415–2419.
- (12) Lynch, C. J.; Milner, J. Loss of one p53 allele results in four-fold reduction of p53 mRNA and protein: A basis for p53 haplo-insufficiency. *Oncogene* **2006**, *25*, 3463–3470.
- (13) Hollstein, M.; Sidransky, D.; Vogelstein, B.; Harris, C. C. p53 mutations in human cancers. *Science* **1991**, *253*, 49–53.
- (14) Farhana, L.; Dawson, M. I.; Leid, M.; Wang, L.; Moore, D. D.; Liu, G.; Xia, Z.; Fontana, J. A. Adamantyl-substituted retinoid-related molecules bind small heterodimer partner and modulate the Sin3A repressor. *Cancer Res.* **2007**, *67*, 318–325.
- (15) Borgius, L. J.; Steffensen, K. R.; Gustafsson, J. A.; Treuter, E. Glucocorticoid signaling is perturbed by the atypical orphan receptor and corepressor SHP. *J. Biol. Chem.* **2002**, *277*, 49761–49766.
- (16) Brendel, C.; Schoonjans, K.; Botrugno, O. A.; Treuter, E.; Auwerx, J. The small heterodimer partner interacts with the liver X receptor alpha and represses its transcriptional activity. *Mol. Endocrinol.* **2002**, *16*, 2065–2076.
- (17) Gobinet, J.; Carascossa, S.; Cavailles, V.; Vignon, F.; Nicolas, J. C.; Jalaguier, S. SHP represses transcriptional activity via recruitment of histone deacetylases. *Biochemistry* **2005**, *44*, 6312–6320.
- (18) Kassam, A.; Capone, J. P.; Rachubinski, R. A. The short heterodimer partner receptor differentially modulates peroxisome proliferator-activated receptor alpha-mediated transcription from the peroxisome proliferator-response elements of the genes encoding the peroxisomal beta-oxidation enzymes acyl-CoA oxidase and hydratase-dehydrogenase. *Mol. Cell. Endocrinol.* **2001**, *176*, 49–56.
- (19) Klinge, C. M.; Jernigan, S. C.; Risinger, K. E.; Lee, J. E.; Tyulmenkov, V. V.; Falkner, K. C.; Prough, R. A. Short heterodimer partner (SHP) orphan nuclear receptor inhibits the transcriptional activity of aryl hydrocarbon receptor (AHR)/AHR nuclear translocator (ARNT). *Arch. Biochem. Biophys.* **2001**, *390*, 64–70.
- (20) Seol, W.; Chung, M.; Moore, D. D. Novel receptor interaction and repression domains in the orphan receptor SHP. *Mol. Cell. Biol.* **1997**, *17*, 7126–7131.
- (21) Yeo, M. G.; Yoo, Y. G.; Choi, H. S.; Pak, Y. K.; Lee, M. O. Negative cross-talk between Nur77 and small heterodimer partner and its role in apoptotic cell death of hepatoma cells. *Mol. Endocrinol.* **2005**, *19*, 950–963.
- (22) Dhanabal, M.; Jeffers, M.; Larochelle, W. J. Anti-angiogenic therapy as a cancer treatment paradigm. *Curr. Med. Chem. Anticancer Agents* **2005**, *5*, 115–130.
- (23) Blagosklonny, M. V. Prospective strategies to enforce selectively cell death in cancer cells. *Oncogene* **2004**, *23*, 2967–2975.
- (24) Fenaux, P.; De Botton, S. Retinoic acid syndrome. Recognition, prevention and management. *Drug Saf.* **1998**, *18*, 273–279.
- (25) Cheer, S. M.; Foster, R. H. Alitretinoin. *Am. J. Clin. Dermatol.* **2000**, *1*, 307–314; discussion 315–316.
- (26) Dawson, M. I.; Chan, R. L.; Derdzinski, K.; Hobbs, P. D.; Chao, W. R.; Schiff, L. J. Synthesis and pharmacological activity of 6-[(E)-2-(2,6,6-trimethyl-1-cyclohexen-1-yl)ethen-1-yl]- and 6-(1,2,3,4-tetrahydro-1,1,4,4-tetramethyl-6-naphthyl)-2-naphthalenecarboxylic acids. *J. Med. Chem.* **1983**, *26*, 1653–1656.
- (27) Newton, D. L.; Henderson, W. R.; Sporn, M. B. Structure-activity relationships of retinoids in hamster tracheal organ culture. *Cancer Res.* **1980**, *40*, 3413–3425.
- (28) Strickland, S.; Breitman, T. R.; Frickel, F.; Nurrenbach, A.; Hadicke, E.; Sporn, M. B. Structure-activity relationships of a new series of retinoid benzoic acid derivatives as measured by induction of differentiation of murine F9 teratocarcinoma cells and human HL60 promyelocytic leukemia cells. *Cancer Res.* **1983**, *43*, 5268–5272.
- (29) Verma, A. K.; Shapas, B. G.; Rice, H. M.; Boutwell, R. K. Correlation of the inhibition by retinoids of tumor promoter-induced mouse epidermal ornithine decarboxylase activity and of skin tumor promotion. *Cancer Res.* **1979**, *39*, 419–425.
- (30) Sporn, M. B.; Roberts, A. B. Biological methods for analysis and assay of retinoids: Relationships between structure and activity. In *The Retinoids*; Sporn, M. B.; Roberts, A. B.; Goodman, D. S., Eds.; Academic Press, Inc.: Orlando, FL, 1984; Chapter 5, Vol. 1, pp 236–279.
- (31) Schiff, L. J.; Okamura, W. H.; Dawson, M. I.; Hobbs, P. D. Structure-biological activity relationships of new synthetic retinoids on epithelial differentiation of cultured hamster trachea. In *Chemistry and Biology of Synthetic Retinoids*; Dawson, M. I.; Okamura, W. H., Eds.; CRC Press: Boca Raton, FL, 1990; pp 307–363.
- (32) Dawson, M. I.; Chao, W.-R.; Hobbs, P. D.; Delair, T. The inhibitory effects of retinoids on the induction of ornithine decarboxylase and the promotion of tumors in mouse epidermis. In *Chemistry and Biology of Synthetic Retinoids*; Dawson, M. I.; Okamura, W. H., Eds.; CRC Press: Boca Raton, FL, 1990; pp 385–466.
- (33) Cincinelli, R.; Dallavalle, S.; Nannei, R.; Carella, S.; De Zani, D.; Merlini, L.; Penco, S.; Garattini, E.; Giannini, G.; Pisano, C.; Vesci, L.; Carminati, P.; Zucco, V.; Zanchi, C.; Zunino, F. Synthesis and structure-activity relationships of a new series of retinoid-related biphenyl-4-ylacrylic acids endowed with antiproliferative and proapoptotic activity. *J. Med. Chem.* **2005**, *48*, 4931–4946.
- (34) Parrella, E.; Gianni, M.; Fratelli, M.; Barzago, M. M.; Raska, I. J.; Diomede, L.; Kurosaki, M.; Pisano, C.; Carminati, P.; Merlini, L.; Dallavalle, S.; Tavecchio, M.; Rochette-Egly, C.; Terao, M.; Garattini, E. Antitumor activity of the retinoid related molecules, ST1926 and CD437, in F9 teratocarcinoma: Role of retinoic acid receptor γ and retinoid-independent pathways. *Mol. Pharmacol.* **2006**, *70*, 909–924.
- (35) Dawson, M. I.; Hobbs, P. D.; Peterson, V. J.; Leid, M.; Lange, C. W.; Feng, K. C.; Chen, G.; Gu, J.; Li, H.; Kolluri, S. K.; Zhang, X.; Zhang, Y.; Fontana, J. A. Apoptosis induction in cancer cells by a novel analogue of 6-[3-(1-adamantyl)-4-hydroxyphenyl]-2-naphthalene carboxylic acid lacking retinoid receptor transcriptional activation activity. *Cancer Res.* **2001**, *61*, 4723–4730.
- (36) Robertson, K. A.; Emami, B.; Collins, S. J. Retinoic acid-resistant HL-60R cells harbor a point mutation in the retinoic acid receptor ligand-binding domain that confers dominant negative activity. *Blood* **1992**, *80*, 1885–1889.
- (37) Tashima, T.; Kagechika, H.; Tsuji, M.; Fukasawa, H.; Kawachi, E.; Hashimoto, Y.; Shudo, K. Polyenyldiene thiazolidinedione derivatives with retinoid activities. *Chem. Pharm. Bull. (Tokyo)* **1997**, *45*, 1805–1813.
- (38) Ebisawa, M.; Kawachi, E.; Fukasawa, H.; Hashimoto, Y.; Itai, A.; Shudo, K.; Kagechika, H. Novel thiazolidinedione derivatives with retinoid synergistic activity. *Biol. Pharm. Bull.* **1998**, *21*, 547–549.
- (39) Yang, D. Y. 4-Hydroxyphenylpyruvate dioxygenase as a drug discovery target. *Drug News Perspect.* **2003**, *16*, 493–496.
- (40) Renaud, J. P.; Rochel, N.; Ruff, M.; Vivat, V.; Chambon, P.; Gronemeyer, H.; Moras, D. Crystal structure of the RAR- α ligand-binding domain bound to all-trans retinoic acid. *Nature* **1995**, *378*, 681–689.
- (41) Klaholz, B. P.; Mitschler, A.; Belema, M.; Zusi, C.; Moras, D. Enantiomer discrimination illustrated by high-resolution crystal structures of the human nuclear receptor hRAR α . *Proc. Natl. Acad. Sci. U.S.A.* **2000**, *97*, 6322–6327.
- (42) Fontana, J. A.; Dawson, M. I.; Leid, M.; Rishi, A. K.; Zhang, Y.; Hsu, C. A.; Lu, J. S.; Peterson, V. J.; Jong, L.; Hobbs, P.; Chao, W. R.; Shroot, B.; Reichert, U. Identification of a unique binding protein specific for a novel retinoid inducing cellular apoptosis. *Int. J. Cancer* **2000**, *86*, 474–479.
- (43) Shipanova, I. N.; Glomb, M. A.; Nagaraj, R. H. Protein modification by methylglyoxal: Chemical nature and synthetic mechanism of a major fluorescent adduct. *Arch. Biochem. Biophys.* **1997**, *344*, 29–36.

- (44) Richardson, R. M.; Pares, X.; Cuchillo, C. M. Chemical modification by pyridoxal 5'-phosphate and cyclohexane-1,2-dione indicates that Lys-7 and Arg-10 are involved in the p2 phosphate-binding subsite of bovine pancreatic ribonuclease A. *Biochem. J.* **1990**, *267*, 593–599.
- (45) Jiang, Z. Y.; Thorpe, C. Modification of an arginine residue in pig kidney general acyl-coenzyme A dehydrogenase by cyclohexane-1,2-dione. *Biochem. J.* **1982**, *207*, 415–419.
- (46) Miyaura, N.; Suzuki, A. Palladium-catalyzed cross-coupling reactions of organoboron compounds. *Chem. Rev.* **1995**, *95*, 2457–2483.
- (47) Ek, F.; Manner, S.; Wistrand, L. G.; Frejd, T. Synthesis of fused tetrazole derivatives via a tandem cycloaddition and *N*-allylation reaction and parallel synthesis of fused tetrazole amines. *J. Org. Chem.* **2004**, *69*, 1346–1352.
- (48) Mancuso, A. J.; Huang, S.-L.; Swern, D. Oxidation of long-chain and related alcohols to carbonyls by dimethyl sulfoxide "activated" by oxalyl chloride. *J. Org. Chem.* **1978**, *43*, 2480–2482.
- (49) Cho, B. R.; Chajara, K.; Oh, H. J.; Son, K. H.; Jeon, S. J. Synthesis and nonlinear optical properties of 1,3,5-methoxy-2,4,6-tris(styryl)-benzene derivatives. *Org. Lett.* **2002**, *4*, 1703–1706.
- (50) Bouchain, G.; Leit, S.; Frechette, S.; Khalil, E. A.; Lavoie, R.; Moradei, O.; Woo, S. H.; Fournel, M.; Yan, P. T.; Kalita, A.; Trachy-Bourget, M. C.; Beaulieu, C.; Li, Z.; Robert, M. F.; MacLeod, A. R.; Besterman, J. M.; Delorme, D. Development of potential antitumor agents. Synthesis and biological evaluation of a new set of sulfonamide derivatives as histone deacetylase inhibitors. *J. Med. Chem.* **2003**, *46*, 820–830.
- (51) Doyle, M. P.; Siegfried, B.; Dellaria, J. F., Jr. Alkyl nitrile-metal halide deamination reactions. 2. Substitutive deamination of arylamines by alkyl nitrites and copper(II) halides. A direct and remarkably efficient conversion of arylamines to aryl halides. *J. Org. Chem.* **1977**, *42*, 2426–2430.
- (52) Musso, D. L.; Clarke, M. J.; Kelley, J. L.; Boswell, G. E.; Chen, G. Novel 3-phenylprop-2-ynylamines as inhibitors of mammalian squalene epoxidase. *Org. Biomol. Chem.* **2003**, *1*, 498–506.
- (53) Brown, H. C.; Subrahmanyam, C.; Hamaoka, T.; Ravindran, N. Vinylic organoboranes. 13. A convenient stereospecific synthesis of (*Z*)-1-halo-1-alkenes from 1-alkynes via (*E*)-1-alkenylborane derivatives with halogens. *J. Org. Chem.* **1989**, *54*, 6068–6075.
- (54) Simoni, D.; Rossi, M.; Rondanin, R.; Mazzali, A.; Baruchello, R.; Malagutti, C.; Roberti, M.; Invidiata, F. P. Strong bicyclic guanidine base-promoted Wittig and Horner–Wadsworth–Emmons reactions. *Org. Lett.* **2000**, *2*, 3765–3768.
- (55) Miyano, M.; Dorn, C. R.; Mueller, R. A. Prostaglandins. IV. A synthesis of F-type prostaglandins. A total synthesis of prostaglandin F₁. *J. Org. Chem.* **1972**, *37*, 1810–1818.
- (56) Zabell, A. P.; Corden, S.; Helquist, P.; Stauffacher, C. V.; Wiest, O. Inhibition studies with rationally designed inhibitors of the human low molecular weight protein tyrosine phosphatase. *Bioorg. Med. Chem.* **2004**, *12*, 1867–1880.
- (57) Palacios, F.; Aparicio, D.; Vicario, J. Synthesis of quinolinylphosphane oxides and -phosphonates from *N*-arylimines derived from the phosphane oxides and phosphonates. *Eur. J. Org. Chem.* **2002**, 4131–4136.
- (58) Klicic, J.; Friesner, F.; Liu, S.-Y.; Guida, W. Accurate prediction of acidity constants in aqueous solution via density functional theory and self-consistent reaction field methods. *J. Phys. Chem. A* **2002**, *106*, 1327–1335.
- (59) Li, H.; Kolluri, S. K.; Gu, J.; Dawson, M. I.; Cao, X.; Hobbs, P. D.; Lin, B.; Chen, G.; Lu, J.; Lin, F.; Xie, Z.; Fontana, J. A.; Reed, J. C.; Zhang, X. Cytochrome c release and apoptosis induced by mitochondrial targeting of nuclear orphan receptor TR3. *Science* **2000**, *289*, 1159–1164.
- (60) Zhang, Y.; Huang, Y.; Rishi, A. K.; Sheikh, M. S.; Shroot, B.; Reichert, U.; Dawson, M.; Poirer, G.; Fontana, J. A. Activation of the p38 and JNK/SAPK mitogen-activated protein kinase pathways during apoptosis is mediated by a novel retinoid. *Exp. Cell. Res.* **1999**, *247*, 233–240.
- (61) Pfahl, M.; Piedrafita, F. J. Retinoid targets for apoptosis induction. *Oncogene* **2003**, *22*, 9058–9062.
- (62) Schubert, S.; Lieuw, K.; Rowe, S. L.; Lee, C. M.; Li, X.; Loh, M. L.; Clapp, D. W.; Shannon, K. M. Functional analysis of leukemia-associated PTPN11 mutations in primary hematopoietic cells. *Blood* **2005**, *106*, 311–317.
- (63) Yu, W. M.; Daino, H.; Chen, J.; Bunting, K. D.; Qu, C. K. Effects of a leukemia-associated gain-of-function mutation of SHP-2 phosphatase on interleukin-3 signaling. *J. Biol. Chem.* **2006**, *281*, 5426–5434.
- (64) Zhu, X. Z.; Yu, Y. Z.; Fang, Y. M.; Liang, Y.; Lu, Q. H.; Xu, R. Z. [Overexpression of Shp-2 is associated with the unlimited growth and apoptosis resistance of p210 bcr-abl-mediated chronic myeloid leukemia]. *Zhonghua Yi Xue Za Zhi* **2005**, *85*, 1903–1906.
- (65) Tauchi, T.; Miyazawa, K.; Feng, G. S.; Broxmeyer, H. E.; Toyama, K. A coiled-coil tetramerization domain of BCR-ABL is essential for the interactions of SH2-containing signal transduction molecules. *J. Biol. Chem.* **1997**, *272*, 1389–1394.
- (66) Farhana, L.; Dawson, M. I.; Huang, Y.; Zhang, Y.; Rishi, A. K.; Reddy, K. B.; Freeman, R. S.; Fontana, J. A. Apoptosis signaling by the novel compound 3-Cl-AHPC involves increased EGFR proteolysis and accompanying decreased phosphatidylinositol 3-kinase and AKT kinase activities. *Oncogene* **2004**, *23*, 1874–1884.
- (67) Tchilian, E. Z.; Beverley, P. C. Altered CD45 expression and disease. *Trends Immunol.* **2006**, *27*, 146–153.
- (68) Miyachi, H.; Tanaka, Y.; Gondo, K.; Kawada, T.; Kato, S.; Sasao, T.; Hotta, T.; Oshima, S.; Ando, Y. Altered expression of CD45 isoforms in differentiation of acute myeloid leukemia. *Am. J. Hematol.* **1999**, *62*, 159–164.
- (69) Arsenou, E. S.; Papadimitriou, E. P.; Kliafa, E.; Hountala, M.; Nikolaropoulos, S. S. Effects of retinoic acid steroidal analogs on human leukemic HL60 cell proliferation in vitro and on angiogenesis in vivo. *Anticancer Drugs* **2005**, *16*, 151–158.
- (70) Dawson, M. I.; Zhang, X.-K. Discovery and design of retinoic acid receptor and retinoid X receptor class-and subtype-selective synthetic analogs of all-*trans*-retinoic acid and 9-*cis*-retinoic acid. *Curr. Med. Chem.* **2002**, *9*, 623–637.
- (71) Peterson, V. J.; Barofsky, E.; Deinzer, M. L.; Dawson, M. I.; Feng, K. C.; Zhang, X.-K.; Madduru, M. R.; Leid, M. Mass-spectrometric analysis of agonist-induced retinoic acid receptor γ conformational change. *Biochem. J.* **2002**, *362*, 173–181.
- (72) Rao, A. V. R.; Chakraborty, T. K.; Reddy, K. L.; Rao, A. S. An expeditious approach for the synthesis of β -hydroxylaryl α -amino acids present in vancomycin. *Tetrahedron Lett.* **1994**, *35*, 5043–5046.
- (73) Wittenberger, S. J.; Donner, B. G. Dialkyltin oxide mediated addition of trimethylsilyl azide to nitriles. A novel preparation of 5-substituted tetrazoles. *J. Org. Chem.* **1993**, *58*, 4139–4141.
- (74) Harris, D. L.; DeLorey, T. M. Determinants of recognition of ligands binding to benzodiazepine receptor/GABA_A receptors initiating sedation. *Eur. J. Pharmacol.* **2000**, *401*, 271–287.
- (75) Harris, D. L.; Loew, G. H. Development and assessment of a 3D pharmacophore for ligand recognition of BDZR/GABA_A receptors initiating the anxiolytic response. *Bioorg. Med. Chem.* **2000**, *8*, 2527–2538.
- (76) Stewart, J. J. P. A semiempirical molecular orbital program. MOPAC. *J. Comput.-Aided Mol. Des.* **1990**, *4*, 1–105.
- (77) Frisch, M. J.; Trucks, G. W.; Schlegel, H. B.; Scuseria, G. E.; Robb, M. A.; Cheeseman, J. R.; Montgomery, J. A., Jr.; Vreven, T.; Kudin, K. N.; Burant, J. C.; Millam, J. M.; Iyengar, S. S.; Tomasi, J.; Barone, V.; Mennucci, B.; Cossi, M.; Scalmani, G.; Rega, N.; Petersson, G. A.; Nakatsuji, H.; Hada, M.; Ehara, M.; Toyota, K.; Fukuda, R.; Hasegawa, J.; Ishida, M.; Nakajima, T.; Honda, Y.; Kitao, O.; Nakai, H.; Klene, M.; Li, X.; Knox, J. E.; Hratchian, H. P.; Cross, J. B.; Bakken, V.; Adamo, C.; Jaramillo, J.; Gomperts, R.; Stratmann, R. E.; Yazyev, O.; Austin, A. J.; Cammi, R.; Pomelli, C.; Ochterski, J. W.; Ayala, P. Y.; Morokuma, K.; Voth, G. A.; Salvador, P.; Dannenberg, J. J.; Zakrzewski, V. G.; Dapprich, S.; Daniels, A. D.; Strain, M. C.; Farkas, O.; Malick, D. K.; Rabuck, A. D.; Raghavachari, K.; Foresman, J. B.; Ortiz, J. V.; Cui, Q.; Baboul, A. G.; Clifford, S.; Cioslowski, J.; Stefanov, B. B.; Liu, G.; Liashenko, A.; Piskorz, P.; Komaromi, I.; Martin, R. L.; Fox, D. J.; Keith, T.; Al-Laham, M. A.; Peng, C. Y.; Nanayakkara, A.; Challacombe, M.; Gill, P. M. W.; Johnson, B.; Chen, W.; Wong, M. W.; Gonzalez, C.; Pople, J. A. *Gaussian 03, Revision C.02*, Gaussian, Inc., Wallingford, CT, 2004.
- (78) Nangia-Makker, P.; Honjo, Y.; Sarvis, R.; Akahani, S.; Hogan, V.; Pienta, K. J.; Raz, A. Galectin-3 induces endothelial cell morphogenesis and angiogenesis. *Am. J. Pathol.* **2000**, *156*, 899–909.